Macroscopic Noisy Bounded Confidence Models with Distributed Radical Opinions

Macroscopic Noisy Bounded Confidence Models with Distributed Radical Opinions

M. A. S. Kolarijani, A. V. Proskurnikov, and P. Mohajerin Esfahani

***Abstract*—In this article, we study the nonlinear Fokker-Planck (FP) equation that arises as a mean-field (macroscopic) approximation of bounded confidence opinion dynamics, where opinions are influenced by environmental noises and opinions of radicals (stubborn individuals). The distribution of radical opinions serves as an infinite-dimensional exogenous input to the FP equation, visibly influencing the steady opinion profile. We establish mathematical properties of the FP equation. In particular, we (i) show the well-posedness of the dynamic equation, (ii) provide existence result accompanied by a quantitative global estimate for the corresponding stationary solution, and (iii) establish an explicit lower bound on the noise level that guarantees exponential convergence of the dynamics to stationary state. Combining the results in (ii) and (iii) readily yields the *input-output stability* of the system for sufficiently large noises. Next, using Fourier analysis, the structure of opinion clusters under the uniform initial distribution is examined. The results of analysis are validated through several numerical simulations of the continuum-agent model (partial differential equation) and the corresponding discrete-agent model (interacting stochastic differential equations) for a particular distribution of radicals.**

***Index Terms*—Opinion dynamics, mean-field models, stochastic systems, nonlinear systems.**

I. Introduction

RECENT decades have witnessed enormous progress in study of complex systems and their system-theoretic properties [1], [2]. The main effort has been invested into study of "self-organization" and "spontaneous order" phenomena [3] that have inspired the development of synchronization and consensus theory [4], [5]. Paradoxically, these regular behaviors arising from local interactions between subsystems (agents, nodes) of a complex system are studied much better than various "irregular" dynamic effects such as persistent disagreement and clustering, exhibited by many real-world systems. Although some culprits of this asynchrony and dissent (e.g. symmetries and other special structures in the coupling mechanisms, exogenous forces acting on some nodes, heterogeneous dynamics of nodes, etc.) have been revealed in the literature [6]–[10], only a few mathematical models have been proposed that are sufficiently "rich" to capture the diversity of clustering behaviors in real-world networks and, at the same time, admit rigorous analysis. Long before the recent "boom" in complex systems, the lack of such models was realized in mathematical sociology. The problem of disclosing mechanisms preventing consensus and maintaining enduring disagreement between individuals [11] is nowadays referred to as the community cleavage problem or Abelson's diversity puzzle [12], [13]. The interdisciplinary area of sociodynamical modeling [13]–[20] has attracted enormous attention of the research community and is primarily concerned with mechanisms of *opinion formation* under social influence.

Only few models, proposed in the literature to describe opinion formation processes, have been secured by experimental evidence. Such models, however, play an important role and contribute, in various aspects, in comprehending complex systems' behaviors such as birth, death and evolution of clusters in systems of interacting particles, and in developing algorithms for control of these behaviors. This explains explosion of interest in models of "opinion formation" in systems and control literature. From the control-theoretic prospect, most of these models are simply networks of interacting agents, obeying the first-order integrator model. However, the term "opinion" is now widespread and used to denote the scalar or multi-dimensional state of an agent, even if this state does not have a clear sociological interpretation[1] (belonging, e.g., to an abstract manifold [21]). The opinion is thus some value of interest, held by an agent and updated, based on displayed opinions of the other agents.

Nowadays, linear models of opinion dynamics, extending the classical French-DeGroot system in various directions (allowing, e.g., stubborn agents, asynchronous interactions and repulsion of opinions [13], [17], [22], [23]) have been thoroughly studied. These models are sufficient to explain consensus and disagreement in social groups, as well as formation of special opinion profiles (e.g., bimodal distributions, standing for opinion polarization), however, general mechanisms leading to emergence and destruction of unequal clusters are still far from being well understood. To explain them, more complicated *nonlinear* models have been proposed, mimicking some important features of social influence. One feature observed in social and biological systems is the *homophily* [24], or tendency of individuals to bond with similar ones. Homophily is related to *biased assimilation* [25] effects: individuals readily accept opinions consistent with their views and tend to dismiss and discount opinions contradicting to their own views. Mathematically, coupling between close opinions is stronger than that of distant opinions, which is modeled by introducing *opinion-dependent* influence weights.

M.A.S. Kolarijani and P. Mohajerin Esfahani are with Delft Center for Systems and Control, Delft University of Technology, Delft, The Netherlands. Email: {M.A.SharifiKolarijani, P.MohajerinEsfahani}@tudelft.nl.

A.V. Proskurnikov is with Department of Electronics and Telecommunications, Politecnico di Torino, Turin, Italy and also with the Institute for Problems of Mechanical Engineering, Russian Academy of Sciences (IPME RAS). Email: anton.p.1982@ieee.org

[1]From the sociological viewpoint, opinions are cognitive orientations of individuals towards some objects or topics [13].

Although the possibility of such nonlinearities in opinion dynamics models was mentioned in the pioneering work [11], substantial progress has been primarily achieved in analysis of *bounded confidence* models proposed several decades later as extensions of the deterministic [26] and randomized gossip-based [27] consensus algorithms for multi-agent networks. Bounded confidence models stipulate that a social actor is insensitive to opinions beyond its bounded *confidence set* (usually, this set is an open or closed ball, centered at the actor's own opinion), which makes the graph of interactions among the agents *distance-dependent*. A detailed survey of bounded confidence models and relevant mathematical results can be found in [18]. Bounded confidence models exhibit convergence of the opinions to some steady values, which can reach consensus or split into several disjoint clusters. If the state-dependent interaction graph of the system is symmetric, this follows from general properties of iterative averaging procedures, and can alternatively be proved by exploring a special Lyapunov function ("kinetic energy") [18], [28], [29]. In the general case of *asymmetric* interaction graphs, such a convergence has been proved only in special situations [29], [30], but seems to be a generic behavior [30]–[32].

Opinions in real social groups, however, usually do not terminate at steady values yet oscillate, which is usually explained by two factors. The first reason explaining opinion fluctuation is exogenous influence, which can be interpreted as some "truth" available to some individuals [33] or a position shared by a group of close-minded opinion leaders or stubborn individulas ("radicals") [34]–[36]. Important results on stability of the HK model with radicals and more general "inertial" bounded confidence models were obtained in [30]. Typically, the exogenous signal is supposed to change slowly compared to the opinion evolution and is thus replaced by a constant; the main concern is the dependence between the constant input and the resulting opinion profile. Numerical results, reported in [34], [35] demonstrate high sensitivity of the opinion clusters to the radical's opinion and reveal some counter-intuitive effects, e.g., an increase in the number of radicals sometimes *decreases* the number of their followers. The second culprit of persistent opinion fluctuation is uncertainty in the opinion dynamics, usually modeled as a random drift of each opinion. The presence of a random excitation can be interpreted as "free will" and unpredictability of a human's decision [37]; besides this, randomized opinion dynamics models are broadly adopted in statistical physics [38]–[41] to study phase transitions in systems of interacting particles.

Even for the classical models from [26], [27], disclosing the relation between the initial and the terminal opinion profiles remains a challenging problem (including, e.g., the $2R$-conjecture [42], [43]). In presence of noise, the analysis becomes even more difficult; some progress in the study of the interplay between confidence range and noise level has been achieved in recent works [44], [45]. One of the important directions in analysis of bounded confidence models is examination of their *asymptotic* properties as the number of social actors becomes very large $N \to \infty$ and their individual opinions are replaced by infinitesimal "elements". The arising *macroscopic* approximations of agent-based models describe the evolution of the distribution of opinion (usually supposed to have a density) and are referred to as density-based [46], continuum-agent [47], [48], Eulerian [49], [50], kinetic [51], hydrodynamical [28] or mean-field [43], [52] models of opinion formation. In the continuous-time situation, the density obeys a nonlinear *Fokker-Planck* (FP) equation. To study clustering behavior of the macroscopic bounded confidence models, efficient numerical methods have been proposed that are based on Fourier analysis [40], [43], [53].

From practical viewpoint, it is convenient to consider opinions staying in a predefined interval, e.g., $[0, 1]$. The HK and Deffuant-Weisbuch (DW) models, as well as their continuous-time counterparts [18], imply that starting within the interval, opinions never escape from it. This property, however, is destroyed by arbitrarily small noises. To keep the opinions bounded, some "boundary conditions" are usually introduced. The *absorbing* boundary condition assumes that the opinions are saturated at the extreme values 0 and 1 [40], [45]; an important result from [45] demonstrates that arbitrarily small noises in this situation destroy clusters and lead to approximate consensus (the maximal deviation of opinions is proportional to the noise level). More interesting are opinion dynamics with the *periodic* boundary condition, wrapping the interval $[0, 1]$ into a circle. The opinion density on the circle corresponds to a 1-*periodic* solution of the FP equation on the real line [43], [53], [54]. A disadvantage of the simple periodic boundary condition is the merging of two extreme opinion values 0 and 1. To distinguish between these extreme opinions, we incorporate an "almost reflective" (precisely, an *even* 2-*periodic*) boundary condition. Dealing with the macroscopic FP equation, the opinion density is then conveniently represented by an even 2-periodic solution on the real line. This paper is primarily concerned with mathematical properties of such solutions.

Main Contributions. In this article, we advance the theory of macroscopic modeling of bounded confidence dynamics. We consider a bounded confidence model with environmental noise which also includes radical opinions, which are not concentrated at a single point (as in [33], [34], [49]) but rather distributed over the interval $[0, 1]$. The FP equation acquires an (infinite-dimensional) exogenous *input*, describing the density and the total mass of the radical opinions. This setup allows us to consider the interplay between the noise and the distributed radicals concerning the behavior of the system. In particular, for the macroscopic FP equation,

(i) the criteria for the existence, uniqueness, and regularity of an even periodic solution are establish (Theorem II.1);
(ii) the existence of stationary solution is studied and a global estimate is provided that bounds the deviation of the stationary state from the uniform distribution (Theorem II.2);
(iii) a sufficient condition is presented for exponential convergence of the dynamics to stationary state (Theorem II.3), entailing (in combination with (ii)) also the input-output stability of the system (Corollary II.4).

Developing ideas from [40], [43], [53], we then use Fourier analysis to characterize the clustering behavior of the system

under the uniform initial distribution and some particular distributions of radical opinions. Specifically,

(iv) a numerical scheme is provided to analyze the impact of the noise and the radical opinions density on the number and timing of the initial clustering behavior (Section V-B).

In the preliminary version of this study [55], we reported the results of Theorem II.2 (Estimate) and Theorem II.3 without detailed technical proofs. In this article, we provide the details along with several necessary preparatory lemmas. In [55, Section IV], we also used Fourier Analysis to study the interplay between the relative number (mass) of radical agents (with respect to normal agents) and the critical noise level for order-disorder transition.

The paper in organized as follows. Section II introduces the macroscopic opinion dynamics model in question. Here, we also present our main theoretical results regarding well-posedness and stability of the model. The next two sections are concerned with technical proofs of these results. Section III is devoted to the proof of well-posedness of the dynamics. In Section IV, we examine the properties of the corresponding stationary equation and provide the technical proofs for theoretical results on stability of stationary state. In Section V, Fourier analysis is used for characterization of the clustering behavior of the model. This general scheme is then used in Section VI for a particular distribution of the radical opinions. These results are accompanied by numerical simulations of both the agent-based and the macroscopic models.

Notations. The convolution of two functions f and g is denoted by $f\star g$. We note that in our case, one of the functions has a compact support, so the convolution integral always exists. For a function $f(t,x)$ we use f_x (resp. f_t) to denote the (partial) derivative with respect to (w.r.t.) x (resp. t), so that f_{xx} is the second derivative w.r.t. x. We also use $\partial_x^i f$ for the i-th order derivative w.r.t. x. Let $X=[0,1]$ and $\tilde X=[-1,1]$. We use $\mathcal{P}(X)$ to denote the the space of probability densities on X. That is, $\rho\in\mathcal{P}(X)$ if $\int_X \rho(x)\,\mathrm{d}x=1$ and $\rho(x)\ge 0$ for all $x\in X$. We also use $\mathcal{P}_e(\tilde X)$ to denote the space of probability densities on X, extended evenly to $\tilde X$. That is, $\mathcal{P}_e(\tilde X)$ is the space of all functions $\rho:\tilde X\to[0,\infty)$ such that $\int_X \rho(x)\,\mathrm{d}x=1$ and $\rho(x)=\rho(-x)\ge 0$ for all $x\in\tilde X$. $L^p(\tilde X)$ denotes the Banach space of all measurable functions $f:\tilde X\to\mathbb{R}$ for which the L_p-norm $\|f\|_{L^p(\tilde X)}$ is finite. $H^k(\tilde X)$ for $k\in\mathbb{N}$ is used to denote the Sobolev space $W^{k,2}(\tilde X)$. We use the subscripts *per* (resp. *ep*) to denote the closed subspace of *periodic* (resp. *even periodic*) functions in the corresponding function space. We denote the dual space of $H^1_{per}(\tilde X)$ by $H^{-1}_{per}(\tilde X)$ and we use $\langle\cdot,\cdot\rangle$ to denote the corresponding paring of $H^1_{per}(\tilde X)$ and $H^{-1}_{per}(\tilde X)$. We use $\to$ and $\rightharpoonup$ to denote strong and weak convergences, respectively, in an appropriate Banach space. A brief overview of function spaces relevant to this study is provided in Appendix A.

II. Model Description and Main Results

A. Macroscopic Model of Opinion Formation

The conventional bounded confidence model describes opinion formation process in a network of $N>1$ agents. All agents have the same *confidence range* $R>0$. Agent i's opinion at time $t\ge 0$, denoted by $x_i(t)\in\mathbb{R}$, is (directly) influenced only by the opinions of agents j, such that $|x_j(t)-x_j(t)|\le R$. One of the simplest continuous-time bounded confidence models is as follows [28]

$$\dot x_i(t)=\sum_{j=1}^N \frac{w\big(x_j(t)-x_i(t)\big)}{N},\ w(\xi)=\begin{cases}\xi,\ |\xi|\le R\\ 0,\ |\xi|>R.\end{cases} \tag{1}$$

It can be shown [18] that the opinions obeying the model (1) always converge $x_i(t)\to x_i^s$ as $t\to\infty$, with $w(x_i^s-x_j^s)=0$ for all i,j, corresponding to either consensus or fragmentation of opinions into multiple clusters. Dynamics of real opinions (as well as physical processes, portrayed by "opinion dynamics" models) often do not exhibit convergence to steady values, and the fluctuation of opinions persists. In order to capture this effect, random uncertainties can be introduced into the model mimicking "free will" and unpredictability of a human's decision [37]. The simplest of these uncertainties is an additive random noise. The model (1) is then replaced by the system of nonlinear SDE

$$\mathrm{d}x_i(t)=\frac{1}{N}\sum_{j=1}^N w\big(x_j(t)-x_i(t)\big)\mathrm{d}t+\sigma\mathrm{d}W_i(t), \tag{2}$$

where W_i are independent standard Wiener processes and $\sigma>0$ characterizes the noise level.

Since the dynamics of a stochastic system (2) becomes quite complicated as the number of agents grows, the standard approach to examine it is the *mean-field* (or macroscopic) approximation, considering the opinion profile $(x_i(t))_{i=1}^N$ as a *random sampling* drawn from some (time-varying) probability distribution of the opinion. Precisely, it can be shown [56]–[58] that empirical distributions $N^{-1}\sum_{i=1}^N\delta_{x_i(t)}$ converge (in the weak sense) as $N\to\infty$ to a distribution, whose density $\rho(t,x)$ obeys the FP equation

$$\rho_t=\big(\rho\ (w\star\rho)\big)_x+\tfrac{\sigma^2}{2}\rho_{xx},\quad t\ge 0,\ x\in\mathbb{R}. \tag{3}$$

A natural extension of the bounded confidence dynamics allows the presence of $N_r\ge 1$ *radicals* (stubborn agents, zealots) that do not assimilate others' opinions, however, influence them directly or indirectly. Typically, the radicals' opinions are supposed to be constant (or changing very slowly compared to the opinion formation of "normal" agents). Indexing the "normal" individuals by $i\in\mathcal{I}_n=\{1,\dots,N\}$ and the radicals by $i\in\mathcal{I}_r=\{N+1,\dots,N+N_r\}$, the opinion dynamics becomes as follows

$$\begin{aligned}&\mathrm{d}x_i(t)=\sum_{j=1}^{N+N_r}\frac{w(x_j(t)-x_i(t))}{N}\mathrm{d}t+\sigma\mathrm{d}W_i(t),\ i\in\mathcal{I}_n\\ &\dot x_i(t)=0,\ i\in\mathcal{I}_r.\end{aligned} \tag{4}$$

Often it is supposed that the radicals share a common opinion $x_i\equiv T$ for $i\in\mathcal{I}_r$, which may also be considered as "truth" perceived by some individuals [33] or some exogenous signal [34]. The ratio $M=N_r/N$ can be treated as the relative "weight" or "strength" of this external opinion. More generally, one can assume that the radicals' opinions are spread over $\mathbb{R}$. Supposing that $N,N_r\to\infty$, the relative

mass of the radicals M remains constant, and their empirical distribution $N_r^{-1}\sum_{i=1}^{N_r}\delta_{x_{N+i}}$ converges (in the weak sense) to a distribution with sufficiently smooth density ρ_r, the density of the "normal" opinions obeys the modified FP equation

$$\rho_t = \big(\rho\ (w\star(\rho+M\rho_r))\big)_x + \tfrac{\sigma^2}{2}\rho_{xx},\quad t\geq 0,\ x\in\mathbb{R}. \quad (5)$$

Note that the classical bounded confidence dynamics (1), being a special case of continuous-time consensus protocol, has an important property: the minimal and maximal opinions $\min_i x_i(t)$ and $\max_i x_i(t)$ are, respectively, non-decreasing and non-increasing. In particular, if the initial opinions are confined to some predefined interval, e.g., $x_i(0)\in[0,1]$, then one has $x_i(t)\in[0,1]$ for all $t\geq 0$. The additive noise leads to random drift of the opinion profile, thus destroying the latter important property. Since in practice bounded ranges of opinions are usually considered, the dynamics (2), (4) are usually complemented by *boundary conditions* [40], preventing the opinions from leaving the predefined range.

A typical boundary condition is the *periodic* condition, where the opinion domain $[0,1]$ is wrapped on a circle of circumference 1 (formally, replacing a real opinion value $x\in\mathbb{R}$ by its fractional part $\{x\}=x \mod 1$). A disadvantage of the periodic boundary condition is that there is no distinction between the extreme opinions 0 and 1. In this paper, we address this issue by considering another type of boundary condition, which we call *even 2-periodic*. Precisely, a real opinion $x\in\mathbb{R}$ is replaced by $f(x)$, where f is an even 2-periodic function, such that $f(x)=x$ on $[0,1]$ (and hence $f(x)=-x$ for $x\in[-1,0]$, $f(x)=2-x$ for $x\in[1,2]$ and so on). In other words, we first *evenly* extend the opinion domain $[0,1]$ into the interval $[-1,1]$ and then wrap it on a circle of circumference 2 so that the extreme opinions 0 and 1 correspond to the antipodes of this circle. We note that with this even 2-periodic extension, the "effective" boundary condition experienced by the agents is an *almost reflective* one, that is, when an agent leaves the opinion domain from one end, it is reflected back into the domain from the same end. This is different from the behavior under simple periodic boundary condition where the agents leaving the domain form one end, enter the domain from the other end. However, the introduced boundary condition is "almost" reflective since the even extension causes some *boundary effects*: the influence of more extreme neighbors of opinion values in the R-neighborhood of extreme opinions 0 and 1 is reinforced. This is due to the even extension which introduces more extreme "artificial" neighbors; see Fig. 1.

As discussed in [43], [53], [54], the FP equation (3) under the periodic conditions retains its validity, however, $\rho(t,x)$ is not a probability density on $\mathbb{R}$ but a 1-periodic function $\rho(t,x+1)=\rho(t,x)\geq 0$, such that $\int_0^1\rho(t,x)\mathrm{d}x=1$ (that is, $\rho(t,\cdot)$ serves as a density on the interval $[0,1]$). Similarly, for the even 2-periodic boundary condition, the equation (3) retains its validity when we replace the probability density $\rho(t,x)$ with an even 2-periodic function, that is, $\rho(t,-x)=\rho(t,x)$ and $\rho(t,x+2)=\rho(t,x)$. On the interval $[0,1]$, the function $\rho(t,\cdot)$ again serves as a probability density: $\int_0^1\rho(t,x)\mathrm{d}x=1$. We also assume that the initial density $\rho_0(x)=\rho(0,x)$ and the density of radical opinions $\rho_r(x)$, defined on $[0,1]$, are extended (in the unique possible way) to even 2-periodic functions on $\mathbb{R}$.

In this study, without loss of generality, we take $X=[0,1]$ and $\tilde{X}=[-1,1]$ to be the bounded opinion domain and its even extension, respectively. To summarize the discussion above, the macroscopic model for opinion dynamics considered in this study is fully described by the following PDE

$$\begin{aligned}\rho_t &= (\rho\ G_\rho)_x+\tfrac{\sigma^2}{2}\rho_{xx} && \text{in} && \tilde{X}\times(0,T)\\ \rho(\cdot+2,t) &= \rho(\cdot,t) && \text{on} && \partial\tilde{X}\times(0,T)\\ \rho(x,\cdot) &= \rho_0(x) && \text{on} && \tilde{X}\times\{t=0\},\end{aligned} \quad (6)$$

where

$$G_\rho(x,t) := w(x)\star\big(\rho(x,t)+M\rho_r(x)\big). \quad (7)$$

Note that in (6), we are considering the dynamics over a finite time horizon T for the sake of analysis, however, T can be chosen arbitrarily large. We again emphasize that the initial density ρ_0 and the radical density ρ_r are the unique even 2-periodic extensions of the corresponding densities from X to $\tilde{X}$. In essence, we are considering the same dynamics as in [54] with the extra requirement for ρ_0 (and the newly introduced density ρ_r) to be even. Finally, we note that [59] also provides a detailed treatment of this dynamics (without radicals) for a class of interaction potentials on a torus in higher dimensions.

B. Main Theoretical Results

To recapitulate, we are interested in even 2-periodic solutions of PDE (6), where ρ_0 and ρ_r are even 2-periodic. A natural question arises as to whether the model is well-posed in the sense that every (sufficiently smooth) initial condition ρ_0 and input ρ_r correspond to a unique solution. The affirmative answer is given in the following theorem.

Theorem II.1 (Well-posedness of dynamics)**.** *Let the initial density of normal opinions and the radical opinions density satisfy $\rho_0\in H^3_{ep}(\tilde{X})\cap\mathcal{P}_e(\tilde{X})$ and $\rho_r\in H^2_{ep}(\tilde{X})\cap\mathcal{P}_e(\tilde{X})$, respectively. Then, PDE (6) has a unique, even, strictly positive, classical solution $\rho\in C^1(0,\infty;C^2_{ep}(\tilde{X}))$ such that $\rho(t)\in\mathcal{P}_e(\tilde{X})$ for all $t>0$.*

This result implies that $\rho(t):=\rho(t,\cdot)$ is a (strictly positive) probability density on $X=[0,1]$ for all $t>0$, as required.

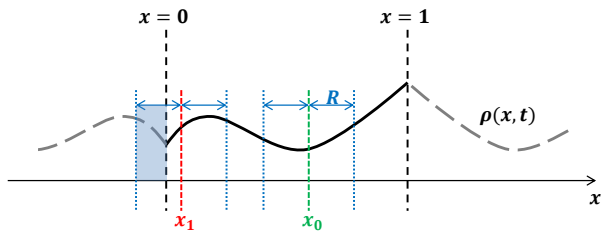

Fig. 1. The even 2-periodic extension of the system. The opinion value $x_0\in[R,1-R]$ effectively experiences a reflective boundary condition, while for the opinion value $x_1\in[0,R]$ there is also a boundary effect due to the even extension. In particular, the influence of more extreme neighbors of x_1 is reinforced by introducing artificial ones (the shaded area in blue). The same boundary effect exists for opinion values in $[1-R,1]$.

For the autonomous systems (without radicals), [54], [59] provide a sufficient condition for exponential convergence of the dynamics towards uniform distribution $\rho = 1$ as an equilibrium of the system. Unlike those studies, the uniform distribution is not an equilibrium of the model considered in this study. However, it is possible to extend this stability result to our model including the exogenous input, i.e., the radicals. To this end, we first consider the stationary equation corresponding to PDE (6) given by

$$\frac{\sigma^2}{2}\rho_{xx} + (\rho\, G_\rho)_x = 0. \tag{8}$$

We are particularly interested in even stationary solutions $\rho^s \in \mathcal{P}_e(\tilde{X})$ of (8). Our next result characterizes the stationary state of the system.

Theorem II.2 (Stationary behavior)**.** *Let $\rho_r \in H^1_{ep}(\tilde{X}) \cap \mathcal{P}_e(\tilde{X})$ be the radical opinions density.*

- ***Existence**: the stationary equation* (8) *has an even, strictly positive, classical solution $\rho^s \in C^2_{ep}(\tilde{X}) \cap \mathcal{P}_e(\tilde{X})$.*
- ***Estimate**: for any $\eta > 0$, if $\sigma^2 > \sigma_b^2 + \eta c_b$, then*

$$\|\rho^s - 1\|_{L^2} \leq \frac{1}{\eta}\, \|\rho_r\|_{L^2},$$

where

$$\sigma_b^2 := \frac{4R}{\pi}\left(M + \frac{R}{\sqrt{3}} + 2\right) \text{ and } c_b := \frac{4R^2 M}{\pi\sqrt{3}}. \tag{9}$$

Notice how the global estimate in Theorem II.2 bounds the difference between the stationary solution and the uniform distribution. This result shows that, even in presence of radical opinions, the stationary solution can be made arbitrarily close to the uniform distribution by increasing the noise level beyond a minimum level σ_b. We note that the minimum noise level σ_b is directly related to the confidence range R and the relative mass M. Moreover, as the "energy" $M\|\rho_r\|_{L^2}$ of the radicals increases, in order to counteract their effect and keep the stationary profile in a somewhat uniform state, one must increase the noise level further beyond σ_b.

With this result in hand, we can now consider the asymptotic stability of stationary state. The next result provides a sufficient condition for exponential convergence of the dynamics to stationary state for arbitrary (and sufficiently smooth) initial density ρ_0 and radical density ρ_r.

Theorem II.3 (Stability)**.** *Let $\rho_0 \in H^3_{ep}(\tilde{X}) \cap \mathcal{P}_e(\tilde{X})$ be the initial density of normal opinions and $\rho_r \in H^2_{ep}(\tilde{X}) \cap \mathcal{P}_e(\tilde{X})$ be the radical opinions density. Also, let $\rho \in C^1(0,\infty; C^2_{ep}(\tilde{X}))$ with $\rho(t) \in \mathcal{P}_e(\tilde{X})$ be the solution to the dynamic equation* (6)*. Then, $\rho(t)$ converges to a stationary state $\rho^s \in C^2_{ep}(\tilde{X}) \cap \mathcal{P}_e(\tilde{X})$ exponentially in L^2 as $t \to \infty$ if $\sigma > \sigma_s$, where $\sigma_s > 0$ uniquely solves*

$$\sigma_s^2 = \frac{4R(3+M)}{\pi} + \frac{4R^2}{\pi\sqrt{3}}\, \exp\left(\frac{8R(1+M)}{\sigma_s^2}\right). \tag{10}$$

An immediate result of Theorems II.2 and II.3 is that for sufficiently large noises, the dynamics will converge to a stationary state that can be made arbitrarily close to uniform distribution by increasing the noise level.

Corollary II.4 (Input-output stability)**.** *For any $\eta > 0$, if $\sigma^2 > \max\{\sigma_b^2 + \eta c_b, \sigma_s^2\}$, where σ_b and c_b are defined in* (9) *and $\sigma_s > 0$ uniquely solves* (10)*, then it holds that*

$$\|\rho(t) - 1\|_{L^2} \leq \beta e^{-\lambda t} + \frac{1}{\eta}\|\rho_r\|_{L^2}, \tag{11}$$

where the constant $\beta > 0$ depends on ρ_0 and ρ_r, and the convergence rate $\lambda > 0$ depends on σ, R, and M.

Remark II.5 (Connection to existing works)**.** *The stability result of Corollary II.4 corresponds to the result reported in [54, Theorem 2.3] on global stability of uniform distribution $\rho = 1$ for sufficiently large noises in the autonomous system* without radicals*. In particular, by setting $M = 0$ in the estimate given in Theorem II.2, one has $c_b = 0$, hence $\rho^s = 1$ is the unique stationary state of the system for $\sigma^2 > \sigma_b^2 = \frac{4R}{\pi}\left(2 + R/\sqrt{3}\right)$. We note that σ_b is the same minimum noise level given in [54, Theorem 2.3], taking into account a multiplicative factor of two due to the even extension considered in this study. However, direct application of Theorem II.3 for stability of $\rho^s = 1$ leads to a sufficient minimum noise level $\sigma_s > \sigma_b$. This is due to the fact that this result is based on conservative estimates for ρ^s. Indeed, if one incorporates the fact that $\rho^s = 1$ and modifies some of the arguments provided in the proof of Theorem II.3 in Section IV-C, then one can show that, in the absence of radical agents, the uniform distribution $\rho^s = 1$ is also globally exponentially stable for $\sigma > \sigma_b$, reproducing the result of [54, Theorem 2.3].*

Finaly, we note that, based on the results provided in [59], the input-output stability result of Corollary II.4 can be generalized to multi-dimensional first-order stochastic interacting particle systems for a particular class of interaction potentials.

The next two sections are mainly concerned with the technical proofs of the theoretical results listed above.

III. Well-posedness of Dynamics

This section is devoted to the proof of Theorem II.1 concerning the well-posedness of the dynamics (6). Throughout this section, all the norms are w.r.t. $\tilde{X} = [-1, 1]$ (as opposed to $X = [0, 1]$), unless indicated otherwise. We use $C, C_0, C_1, \ldots$ to represent a generic constant (depending on the model parameters) which actual values may change from line to line. In case these constants depend on a particular object of interest, say θ, this dependence is explicitly indicated by $C[\theta]$.

Let us first note that because of periodicity, the mass is preserved in (6), that is, $\int_{\tilde{X}} \rho(x,t)\, \mathrm{d}x = \int_{\tilde{X}} \rho_0(x)\, \mathrm{d}x = 2$, for all $t \geq 0$. In particular, we have

$$\|\rho(t)\|_{L^1} \geq \int_{\tilde{X}} \rho(x,t)\, \mathrm{d}x = 2 > 0.$$

We will be using this property in the sequel.

We begin with presenting some useful estimates for the object G_ρ defined in (7) that make it possible to extend the results provided by [54] to our model.

Lemma III.1 (Estimates for G_ρ)**.** *Let G_ρ be the function defined in* (7) *with $\rho_r \in \mathcal{P}_e(\tilde{X})$. If $\rho(t) \in L^1_{per}(\tilde{X})$, then*

$$\|G_\rho\|_{L^\infty} \leq R\left(\|\rho(t)\|_{L^1} + 2M\right). \tag{12}$$

If, moreover, $\|\rho(t)\|_{L^1} > 0$ *, then*

$$\|G_\rho\|_{L^\infty} \le C \ \|\rho(t)\|_{L^1} \le C \ \|\rho(t)\|_{L^2}. \tag{13}$$

Proof. See the proof of [60, Lemma 3.1]. □

Using the estimate (13) in Lemma III.1, one can follow similar arguments as in [54, Lemma 2.1] to show $\|\rho(t)\|_{L^1} = 2$ and $\rho(t) \ge 0$ for all $t \ge 0$; see also [54, Corollary 2.2]. Specifically, assuming PDE (6) has a solution $\rho \in C^1(0,T;C^2_{per}(\tilde{X}))$, one can derive a priori estimate which in turn implies that the solution is *non-negative* so that $\rho(t)$ is a probability distribution on $X = [0,1]$ for all $t \ge 0$. We will be using these a priori properties in the sequel.

Lemma III.2 (Estimates for $\partial_x^k G_\rho$)**.** *Let* G_ρ *be the function defined in* (7) *with* $\rho_r \in \mathcal{P}_e(\tilde{X})$.

(i) *For* $1 \le p \le \infty$*, if* $\rho(t), \rho_r \in L^p_{per}(\tilde{X})$ *with* $\|\rho(t)\|_{L^1} > 0$*, then*

$$\begin{aligned}\|(G_\rho)_x\|_{L^p} &\le C_1 \ \|\rho(t)\|_{L^p} + C_2 \ \|\rho_r\|_{L^p} \\ &\le C[\|\rho_r\|_{L^p}] \ \|\rho(t)\|_{L^p}.\end{aligned} \tag{14}$$

(ii) *For* $k \ge 2$*, if* $\rho(t), \rho_r \in H^{k-1}_{per}(\tilde{X})$ *with* $\|\rho(t)\|_{L^1} > 0$*, then*

$$\|\partial_x^k G_\rho\|_{L^2} \le C[\|\rho_r\|_{H^{k-1}}] \ \|\rho(t)\|_{H^{k-1}}. \tag{15}$$

Proof. See the proof of [60, Lemma 3.2].. □

The next Lemma extends [54, Proposition 4.1] for our system including exogenous input.

Lemma III.3 (More estimates for G_ρ)**.** *Let* $\nu \in H^k_{per}(\tilde{X})$*,* $\rho_r \in H^{k-1}_{per}(\tilde{X}) \cap \mathcal{P}_e(X)$*, and* $\rho(t) \in H^{k-1}_{per}(\tilde{X})$ *with* $\|\rho(t)\|_{L^1} > 0$*. Then, for* $k \ge 2$*,*

$$\|\nu G_\rho\|_{H^k} \le C[\|\rho_r\|_{H^{k-1}}] \ \|\nu\|_{H^k} \ \|\rho(t)\|_{H^{k-1}}. \tag{16}$$

Proof. See the proof of [60, Lemma 3.3]. □

With these estimates in hand, we can follow the same arguments as in [54] to show well-posedness of the dynamics described by PDE (6). In the sequel we provide the sketch of the proof of Theorem II.1. For a more detailed version, see [60, Section 3].

Proof sketch for Theorem II.1. Consider the PDE sequence

$$\begin{aligned}(\rho_n)_t = (\rho_n G_{\rho_{n-1}})_x + \tfrac{\sigma^2}{2}(\rho_n)_{xx} \quad &\text{in } \tilde{X} \times (0,T) \\ \rho_n(\cdot+2,t) = \rho_n(\cdot,t) \quad &\text{on } \partial\tilde{X} \times (0,T) \\ \rho_n(x,\cdot) = \rho_0(x) \quad &\text{on } \tilde{X} \times \{t=0\},\end{aligned} \tag{17}$$

with smooth data $\rho_0, \rho_r \in C^\infty_{per}(\tilde{X}) \cap \mathcal{P}_e(\tilde{X})$ for now. By standard results on linear parabolic PDEs [61, Chapter 7], there exists a sequence $\{\rho_n : n \ge 0\}$ in $C^\infty(0,T;C^\infty_{per}(\tilde{X}))$ that satisfies (17). Furthermore, using the estimate (13) in Lemma III.1, one can follow the same procedure provided in [54, Proposition 3.1] to show $\|\rho_n(t)\|_{L^1} = \|\rho_n(0)\|_{L^1} = 2$, and hence, $\rho_n(t) \ge 0$ for all $n \ge 1$ and $t \ge 0$; see also [54, Corollary 3.2].

Remark III.4 (Evenness of ρ_n)**.** *One can use the evenness of* ρ_0 *and* ρ_r *to show that the unique solutions* ρ_n *to PDEs* (17) *are also even in* x *for all* $t \ge 0$*. However, since this property will not be used for existence, uniqueness and regularity results provided below, we will postpone this argument to later when we deal with the evenness of the unique solution to PDE* (6)*.*

Existence with smooth data. Using Lemmas III.1 and III.2 and following a similar idea as in [54, Lemmas 3.5 and 3.7], we can obtain the following convergence results for a limiting object $\bar{\rho}$

$$\begin{aligned}\rho_n \to \bar{\rho} \quad &\text{in} \quad L^1(0,T;L^1_{per}(\tilde{X})), \\ \rho_{n_k} \rightharpoonup \bar{\rho} \quad &\text{in} \quad L^2(0,T;H^1_{per}(\tilde{X})), \\ \partial_t \rho_{n_k} \rightharpoonup \bar{\rho}_t \quad &\text{in} \quad L^2(0,T;H^{-1}_{per}(\tilde{X})),\end{aligned} \tag{18}$$

where n_k denotes a subsequence. Moreover, we have the following estimate for $\{\rho_n : n \ge 1\}$ and $\bar{\rho}$

$$\begin{aligned}\|\rho\|_{L^\infty(0,T;L^2)} + \|\rho\|_{L^2(0,T;H^1)} + \|\rho_t\|_{L^2(0,T;H^{-1})} \\ \le C[T] \ \|\rho_0\|_{L^2}.\end{aligned} \tag{19}$$

We claim that $\bar{\rho}$ is the unique weak solution to (6). That is, $\bar{\rho}$ solves the weak formulation of (6) defined as

$$\int_0^T \langle \eta, \rho_t \rangle \ \mathrm{d}t + \int_0^T \int_{\tilde{X}} \left(\tfrac{\sigma^2}{2}\rho_x + \rho \ G_\rho \right) \ \eta_x \ \mathrm{d}x\mathrm{d}t = 0, \tag{20}$$

for any $\eta \in L^2(0,T;H^1_{per}(\tilde{X}))$. To this end, we multiply (17) by η with $n = n_k$ and integrate to obtain

$$\begin{aligned}\int_0^T \langle \eta, \partial_t \rho_{n_k} \rangle \ \mathrm{d}t + \frac{\sigma^2}{2} \int_0^T \int_{\tilde{X}} \partial_x \rho_{n_k} \ \eta_x \ \mathrm{d}x\mathrm{d}t \\ + \int_0^T \int_{\tilde{X}} \rho_{n_k} \ G_{\rho_{n_k-1}} \ \eta_x \ \mathrm{d}x\mathrm{d}t = 0.\end{aligned} \tag{21}$$

Using the convergence results (18) and the estimate (19), one can show that limits of the three terms in (21) are zero as $k \to \infty$, that is, $\bar{\rho}$ indeed satisfies the weak formulation (20). It remains to show $\bar{\rho}(x,0) = \rho_0(x)$. Note that this condition makes sense since $\bar{\rho} \in C(0,T;L^2_{per}(\tilde{X}))$ by [54, Theorem 3.8] and the last two items in convergence results (18). Pick some $\eta \in C^1(0,T;H^1_{per}(\tilde{X}))$ with $\eta(T) = 0$ and rewrite the weak formulation (20) as

$$\begin{aligned}&- \int_0^T \langle \bar{\rho}, \eta_t \rangle \ \mathrm{d}t + \int_0^T \int_{\tilde{X}} \left(\tfrac{\sigma^2}{2}\bar{\rho}_x + \bar{\rho} \ G_{\bar{\rho}} \right) \ \eta_x \ \mathrm{d}x\mathrm{d}t \\ &= \int_{\tilde{X}} \bar{\rho}(x,0) \ \eta(x,0) \ \mathrm{d}x.\end{aligned} \tag{22}$$

Similarly, since $\rho_{n_k}(x,0) = \rho_0(x)$, we have

$$\begin{aligned}&- \int_0^T \langle \rho_{n_k}, \eta_t \rangle \mathrm{d}t + \int_0^T \int_{\tilde{X}} \left(\tfrac{\sigma^2}{2}\partial_x \rho_{n_k} + \rho_{n_k} G_{\rho_{n_k}} \right) \eta_x \mathrm{d}x\mathrm{d}t \\ &= \int_{\tilde{X}} \rho_0(x) \ \eta(x,0) \ \mathrm{d}x.\end{aligned} \tag{23}$$

Let $k \to \infty$ in (23), so for arbitrary $\eta(x,0)$ we obtain from (23) and (22) that

$$\int_{\tilde{X}} \bar{\rho}(x,0) \ \eta(x,0) \ \mathrm{d}x = \int_{\tilde{X}} \rho_0(x) \ \eta(x,0) \ \mathrm{d}x.$$

This implies that $\bar{\rho}(x,0) = \rho_0(x)$.

Relaxed regularity on data. In order to relax regularity assumption on data to $\rho_0, \rho_r \in L^2_{per}(\tilde{X}) \cap \mathcal{P}_e(\tilde{X})$, we can use the mollified version of the distributions $\rho_0^\epsilon = \phi_\epsilon \star \rho_0$ and $\rho_r^\epsilon = \phi_\epsilon \star \rho_r$ with the standard positive mollifier ϕ_ϵ, follow the same procedure and take the limit $\epsilon \to 0$ at the end. See also [54, Theorem 3.12] for the details of this process.

Uniquness. Let $\xi = \bar{\rho}_1 - \bar{\rho}_2$ where $\bar{\rho}_1$ and $\bar{\rho}_2$ are two weak solutions to (6) with $\rho_0, \rho_r \in L^2_{per}(\tilde{X}) \cap \mathcal{P}_e(\tilde{X})$. Then, for every $\eta \in L^2(0,T;H^1_{per}(\tilde{X}))$ we have

$$\begin{aligned}&\int_0^T \langle \eta, \xi_t \rangle \, \mathrm{d}t + \tfrac{\sigma^2}{2} \int_0^T \int_{\tilde{X}} \xi_x \, \eta_x \, \mathrm{d}x\mathrm{d}t \\ &+ \int_0^T \int_{\tilde{X}} (\bar{\rho}_1 \, G_{\bar{\rho}_1} - \bar{\rho}_2 \, G_{\bar{\rho}_2}) \, \eta_x \, \mathrm{d}x\mathrm{d}t \quad = 0.\end{aligned}$$

Setting $\eta = \xi$ and using Lemma III.1, we can follow similar arguments to ones provided in [54, Theorem 3.10] to obtain

$$\int_0^T \langle \xi, \xi_t \rangle \, \mathrm{d}t \leq \left(C_1 + C_2[T] \, \|\rho_0\|^2_{L^2}\right) \, \|\xi\|^2_{L^2(0,T;L^2)}.$$

By [54, Theorem 3.8], we know $\langle \xi, \xi_t \rangle = \frac{1}{2} \frac{\mathrm{d}}{\mathrm{d}t} \|\xi(t)\|^2_{L^2}$. Thus, for all T, we have

$$\frac{1}{2} \int_0^T \tfrac{\mathrm{d}}{\mathrm{d}t} \|\xi(t)\|^2_{L^2} \, \mathrm{d}t \leq \left(C_1 + C_2[T] \, \|\rho_0\|^2_{L^2}\right) \, \int_0^T \|\xi(t)\|^2_{L^2} \mathrm{d}t.$$

This implies that, for a.e. $t \in [0,T]$,

$$\frac{\mathrm{d}}{\mathrm{d}t} \|\xi(t)\|^2_{L^2} \leq C[T, \rho_0] \, \|\xi(t)\|^2_{L^2}.$$

Hence, by Grönwall's inequality,

$$\|\xi(t)\|^2_{L^2} \leq C[T, \rho_0] \, \|\xi(0)\|^2_{L^2} = C[T, \rho_0] \, \|\rho_0 - \rho_0\|^2_{L^2} = 0.$$

That is, $\|\xi(t)\|_{L^2} = \|\bar{\rho}_1(t) - \bar{\rho}_2(t)\|_{L^2} = 0$. Then, from continuity of $\bar{\rho}_1$ and $\bar{\rho}_2$ in time (by [54, Theorem 3.8]), we have $\bar{\rho}_1 = \bar{\rho}_2$ for all $t \in [0,T]$.

Regularity. Employing Lemma III.3, we can extend the improved regularity results in space in [54, Theorem 4.2]. That is, for $\rho_0 \in H^k_{per}(\tilde{X}) \cap \mathcal{P}_e(\tilde{X})$ and $\rho_r \in H^{k-1}_{per}(\tilde{X}) \cap \mathcal{P}_e(\tilde{X})$, we have

$$\bar{\rho} \in L^2(0,T;H^{k+1}_{per}(\tilde{X})) \cap L^\infty(0,T;H^k_{per}(\tilde{X})). \tag{24}$$

Moreover, since ρ_r is constant in time, we can also employ the results on improved regularity in time provided by [54, Theorem 4.3] for our model. This means, for $\rho_0 \in H^{2k}_{per}(\tilde{X}) \cap \mathcal{P}_e(\tilde{X})$ and $\rho_r \in L^2_{per}(\tilde{X}) \cap \mathcal{P}_e(\tilde{X})$, we have for $i \leq k$

$$\partial_t^i \bar{\rho} \in L^2(0,T;H^{2k-2i+1}_{per}(\tilde{X})) \cap L^\infty(0,T;H^{2k-2i}_{per}(\tilde{X})), \tag{25}$$

and

$$\partial_t^{k+1} \bar{\rho} \in L^2(0,T;H^{-1}_{per}(\tilde{X})). \tag{26}$$

With these regularity results in space and time, we can derive the required regularity on the solution as stated in Theorem II.1. Let $\rho_0 \in H^3_{per}(\tilde{X}) \cap \mathcal{P}_e(\tilde{X})$ and $\rho_r \in H^2_{per}(\tilde{X}) \cap \mathcal{P}_e(\tilde{X})$ and also let $\bar{\rho}$ be the unique weak solution to PDE (6). By (24), we have $\bar{\rho} \in L^\infty(0,T;H^3_{per}(\tilde{X}))$. Hence, by the Sobolev embedding theorem [62, Section 4.12], we have $\bar{\rho}(t) \in C^2_{per}(\tilde{X})$ (after possibly being redefined on a set of measure zero). This gives the required regularity in space. Also, (25) and (26) imply that $\bar{\rho}_t \in L^2(0,T;H^1_{per}(\tilde{X}))$ and $\bar{\rho}_{tt} \in L^2(0,T;H^{-1}_{per}(\tilde{X}))$. Hence, by [54, Theorem 3.8], we have $\bar{\rho}_t \in C(0,T;L^2_{per}(\tilde{X}))$ (after possibly being redefined on a set of measure zero). This gives the required regularity in time. Putting these results together, we have $\bar{\rho} \in C^1(0,T;C^2_{per}(\tilde{X}))$.

Evenness. The evenness imposed on ρ_0 and ρ_r implies that if $\rho(x,t)$ is a solution of (6), then $\rho(-x,t)$ is also a solution. Then, assuming $\rho_0 \in H^3_{ep}(\tilde{X}) \cap \mathcal{P}_e(\tilde{X})$ and $\rho_r \in H^2_{ep}(\tilde{X}) \cap \mathcal{P}_e(\tilde{X})$ (notice that $H^k_{ep}(\tilde{X}) \subset H^k_{per}(\tilde{X})$), the *uniqueness* of the solution $\bar{\rho} \in C^1(0,T;C^2_{per}(\tilde{X}))$ to PDE (6) implies that the solution is even, that is, $\bar{\rho} \in C^1(0,T;C^2_{ep}(\tilde{X}))$.

Positivity. Using the same approach as in [59], we consider the following version of (6) in the unknown function ρ with $\bar{\rho}$ being the non-negative weak solution

$$\rho_t = (\rho \, G_{\bar{\rho}})_x + \frac{\sigma^2}{2} \rho_{xx}.$$

This is a linear parabolic PDE with smooth and bounded coefficients (by Lemmas III.1 and III.2) for which $\bar{\rho}$ is a classic non-negative solution. Thus, by parabolic Harnack inequality [61, Section 7.1.4, Theorem 10], we have $\sup_{x \in \tilde{X}} \bar{\rho}(x,t_1) \leq c \inf_{x \in \tilde{X}} \bar{\rho}(x,t_2)$ for $0 < t_1 < t_2 < \infty$ and some constant $c > 0$. Non-negativity of $\bar{\rho}(x,t)$ implies that $\inf_{x \in \tilde{X}} \bar{\rho}(x,t)$ and thus $\bar{\rho}(x,t)$ is positive for all $t > 0$. □

IV. Stationary Behavior and Stability

A. Existence of Stationary Solution

This section mainly concerns the proof of *existence* result in Theorem II.2 for stationary equation (8). Throughout this section, the norms are w.r.t. $X = [0,1]$ (as opposed to $\tilde{X} = [-1,1]$), unless indicated otherwise. We note that norms on the even 2-periodic spaces computed w.r.t. to X and $\tilde{X}$ differ by a multiplicative constant, e.g., $\|u\|_{L^p(\tilde{X})} = 2^{\frac{1}{p}} \|u\|_{L^p(X)}$. We again use $C, C_0, C_1, \ldots$ to represent a generic constant which actual values may change from line to line, where $C[\theta]$ denotes the dependence of the constant on a particular object θ.

Let us begin with providing a fixed point characterization of the solution to stationary equation (8). We note that, corresponding to the solution to dynamic equation (6), we are particularly interested in *even* solutions $\rho^s \in \mathcal{P}_e(\tilde{X})$ of stationary equation (8).

Lemma IV.1 (Fixed point characterization)**.** *$\rho^s \in C^2_{ep}(\tilde{X}) \cap \mathcal{P}_e(\tilde{X})$ is a solution of stationary equation* (8) *if and only if ρ^s is a fixed point of the operator $\mathcal{T} : \mathcal{P}_e(\tilde{X}) \to \mathcal{P}_e(\tilde{X})$ defined as*

$$\mathcal{T}\rho := \tfrac{1}{K} \exp\left(-\tfrac{2}{\sigma^2} \int_0^x G_\rho(z) \, \mathrm{d}z\right), \tag{27}$$

where the constant K is determined by the normalizing condition

$$K = \int_0^1 \exp\left(-\tfrac{2}{\sigma^2} \int_0^x G_\rho(z) \, \mathrm{d}z\right) \mathrm{d}x.$$

Proof. See the proof of [60, Lemma 4.1]. □

This characterization allows us to use tools from operator theory, in particular, Schauder fixed point theorem, to show existence of stationary solution. Before that, we present some preliminary results for the operator $\mathcal{T}$.

Lemma IV.2 (Estimates for $\mathcal{T}$)**.** *Let $\mathcal{T}$ be the operator on $\mathcal{P}_e(\tilde{X})$ defined by* (27)*.*

- *If $\rho, \rho_r \in \mathcal{P}_e(\tilde{X})$, then*

$$\|\mathcal{T}\rho\|_{L^\infty} \leq \mathrm{e}^{8R(1+M)/\sigma^2}, \tag{28}$$

and

$$\|\partial_x \mathcal{T}\rho\|_{L^\infty} \leq \frac{4R(1+M)}{\sigma^2} \, \mathrm{e}^{8R(1+M)/\sigma^2}. \tag{29}$$

- *For $k \geq 3$, if $\rho, \rho_r \in H^{k-2}_{ep}(\tilde{X}) \cap \mathcal{P}_e(\tilde{X})$, then*

$$\|\mathcal{T}\rho\|_{H^k} \leq \sum_{i=1}^{k-1} C_i[\|\rho_r\|_{H^{k-2}}] \ \|\rho\|^i_{H^{k-2}}. \tag{30}$$

Proof. See the proof of [60, Lemma 4.2]. □

Proposition IV.3 (Lipschitz continuity of $\mathcal{T}$)**.** *Let $\mathcal{T}$ be the operator on $\mathcal{P}_e(\tilde{X})$ defined by* (27) *with $\rho_r \in \mathcal{P}_e(\tilde{X})$. Then $\mathcal{T}$ is Lipschitz continuous in L^p for $1 \leq p < \infty$ with Lipschitz constant*

$$L_{\mathcal{T}} = \frac{1}{2} \exp\left(\frac{8R(1+M)(p-1)}{\sigma^2 p}\right)\left(\mathrm{e}^{16R/\sigma^2} - 1\right). \tag{31}$$

Proof. See the proof of [60, Proposition 4.3]. □

With this preliminary results in hand, we next move on to the proof of existence of stationary solution.

Proof of Theorem II.2 (Existence). Following the same argument as in [59, Theorem 2.3] and using Lemma IV.1, we can present the existence result for the stationary solution as the fixed point of the operator $\mathcal{T}$. First note that using the estimate (28) in Lemma IV.2, we have $\|\mathcal{T}\rho\|_{L^2} \leq C\,\|\mathcal{T}\rho\|_{L^\infty} \leq c$ for some positive constant c. Thus, for the purpose of finding the fixed points of $\mathcal{T}$, we can restrict $\mathcal{T}$ to act on the closed and convex set $E := \{\rho \in L^2_{ep}(\tilde{X}) \cap \mathcal{P}_e(\tilde{X}) : \|\rho\|_{L^2} \leq c\}$. Now, from inequalities (28) and (29) in Lemma IV.2, we have, for all $\rho \in E$,

$$\begin{aligned}\|\mathcal{T}\rho\|^2_{H^1} &\leq \|\mathcal{T}\rho\|^2_{L^2} + \|\partial_x \mathcal{T}\rho\|^2_{L^2} \\ &\leq C_1\|\mathcal{T}\rho\|^2_{L^\infty} + C_2\|\partial_x\mathcal{T}\rho\|^2_{L^\infty} \leq c',\end{aligned} \tag{32}$$

for some constant $c' > 0$. That is, $\mathcal{T}(E) \subset E$ is uniformly bounded in $H^1_{ep}(\tilde{X})$. Thus, by the Rellich-Kondrachov compactness theorem [61, Section 5.7, Theorem 1], $\mathcal{T}(E)$ is precompact in $L^2_{ep}(\tilde{X})$. Since $E \subset L^2_{ep}(\tilde{X})$ is closed, this implies $\mathcal{T}(E)$ is also precompact in E. Also, $\mathcal{T}$ is Lipschitz continuous by Proposition IV.3. Hence, by Schauder fixed point theorem [61, Section 9.2.2, Theorem 3], it has a fixed point $\rho^s \in E$ which by (32) belongs to $H^1_{ep}(\tilde{X})$.

Regularity. The estimate (30) in Lemma (IV.2) implies that if $\rho_r \in H^{k-2}_{ep}(\tilde{X})$, then the fixed point $\rho^s = \mathcal{T}\rho^s \in H^k_{ep}(\tilde{X})$. In particular, if $\rho_r \in H^1_{ep}(\tilde{X})$, then $\rho^s \in H^3_{ep}(\tilde{X})$. Hence, by Sobolev embedding theorem, $\rho^s \in C^2_{ep}(\tilde{X})$ (after possibly being redefined on a set of measure zero).

Positivity. Strict positivity of the fixed point (stationary solution) immediately follows from the representation (27). □

Remark IV.4 (Uniqueness)**.** *By Proposition IV.3, $\mathcal{T}$ is Lipschitz continuous in L^p with Lipschitz constant $L_{\mathcal{T}}$ given by* (31)*, and thus, is a contraction for $L_{\mathcal{T}} < 1$. Hence, by Banach fixed-point theorem [61, Section 9.2.1, Theorem 1], $\mathcal{T}$ has a unique fixed point for $L_{\mathcal{T}} < 1$. Setting $p = 1$ in* (31) *gives the sufficient condition $\sigma^2 > 16R/\ln 3$ for* uniqueness *of stationary solution. This result corresponds to the sufficient condition provided in [52, Theorem 2].*

B. Global Estimate for Stationary Solution

This section is devoted to the proof of the *estimate* given in Theorem II.2. In this section, all the norms are w.r.t. the domain $\tilde{X} = [-1, 1]$, unless indicated otherwise.

Proof of Theorem II.2 (Estimate). Let $\psi = \rho^s - 1$ so that $\int_{\tilde{X}} \psi(x)\ \mathrm{d}x = 0$. From the stationary equation (8), we obtain

$$-\frac{\sigma^2}{2}\psi_{xx} = [(\psi+1)\ G_{\psi+1}]_x = [\psi\ G_\psi]_x + [G_\psi]_x,$$

where we used the fact that $w \star 1 = 0$. Next, we multiply this last equation by ψ and integrate by part over $\tilde{X}$ to derive (extra terms are zero due to periodicity)

$$\frac{\sigma^2}{2}\|\psi_x\|^2_{L^2} = -\int_{\tilde{X}} \psi_x\ \psi\ G_\psi\ \mathrm{d}x - \int_{\tilde{X}} \psi_x\ G_\psi\ \mathrm{d}x.$$

Thus,

$$\begin{aligned}\frac{\sigma^2}{2}\|\psi_x\|^2_{L^2} &\leq \left|\int_{\tilde{X}} \psi_x\ \psi\ G_\psi\ \mathrm{d}x\right| + \left|\int_{\tilde{X}} \psi_x\ G_\psi\ \mathrm{d}x\right| \\ &\leq \|G_\psi\|_{L^\infty}\ \|\psi_x\|_{L^2}\ \|\psi\|_{L^2} + \|\psi_x\|_{L^2}\ \|G_\psi\|_{L^2}.\end{aligned} \tag{33}$$

Now, using inequality (12) in Lemma III.1, we obtain

$$\begin{aligned}\|G_\psi\|_{L^\infty} &\leq 2R\left(\|\psi\|_{L^1(X)} + M\right) \\ &\leq 2R\left(\|\rho\|_{L^1(X)} + 1 + M\right) \leq 2R(M+2).\end{aligned} \tag{34}$$

Also, we have

$$\begin{aligned}|G_\psi(x)|^2 &= \left(\int_{x-R}^{x+R}(x-y)\ (\psi(y) + M\rho_r(y))\ \mathrm{d}y\right)^2 \\ &\leq \int_{x-R}^{x+R}(x-y)^2\ \mathrm{d}y\ \int_{x-R}^{x+R}(\psi(y) + M\rho_r(y))^2\ \mathrm{d}y \\ &\leq (2/3)R^3 \int_{x-R}^{x+R}(\psi(y) + M\rho_r(y))^2\ \mathrm{d}y.\end{aligned} \tag{35}$$

Hence,

$$\begin{aligned}\|G_\psi\|^2_{L^2} &\leq (2/3)R^3 \int_{\tilde{X}}\int_{x-R}^{x+R}(\psi(y) + M\rho_r(y))^2\ \mathrm{d}y\mathrm{d}x \\ &= (2/3)R^3 \int_{\tilde{X}}\int_{-R}^{R}(\psi(x+y) + M\rho_r(x+y))^2\ \mathrm{d}y\mathrm{d}x \\ &= (4/3)R^4\|\psi + M\rho_r\|^2_{L^2}.\end{aligned} \tag{36}$$

Using estimates (34) and (36) in (33), we have (recall that uniform distribution is not an equilibrium of the system and hence $\|\psi_x\|_{L^2} \neq 0$)

$$\begin{aligned}\frac{\sigma^2}{2}\|\psi_x\|_{L^2} &\leq 2R(M+2)\|\psi\|_{L^2} + (2R^2/\sqrt{3})\|\psi + M\rho_r\|_{L^2} \\ &\leq 2R(M+2)\|\psi\|_{L^2} + (2R^2/\sqrt{3})\left(\|\psi\|_{L^2} + M\|\rho_r\|_{L^2}\right) \\ &= 2R\left(M + \frac{R}{\sqrt{3}} + 2\right)\|\psi\|_{L^2} + \frac{2R^2M}{\sqrt{3}}\|\rho_r\|_{L^2}.\end{aligned} \tag{37}$$

Now, since $\int_{\tilde{X}} \psi(x)\ \mathrm{d}x = 0$, Poincaré inequality [61, Section 5.8.1, Theorem 1] implies that $\|\psi\|_{L^2} \leq C\ \|\psi_x\|_{L^2}$. The optimal value for the Poincaré constant for $\tilde{X} = [-1, 1]$ is $C = 1/\pi$. Using this for inequality (37), we have

$$\left(\sigma^2 - \frac{4R}{\pi}\left(M + \frac{R}{\sqrt{3}} + 2\right)\right)\|\psi\|_{L^2} \leq \frac{4R^2M}{\pi\sqrt{3}}\|\rho_r\|_{L^2}. \tag{38}$$

Defining σ_b and c_b as in (9) gives the desired inequality $\|\psi\|_{L^2} \leq \frac{1}{\eta}\|\rho_r\|_{L^2}$, where $\eta = (\sigma^2 - \sigma_b^2)/c_b$. □

C. Stability of Stationary State

This section is devoted to the proof of Theorem II.3 concerning the stability of stationary state. All the norms in this section are w.r.t. the domain $\tilde{X} = [-1, 1]$ (as opposed to $X = [0, 1]$), unless indicated otherwise.

Proof of Theorem II.3. We follow a similar argument as in [54], except we consider a general stationary state ρ^s, instead of the uniform distribution considered in [54]. Let $\psi = \rho - \rho^s$ so that $\int_{\tilde{X}} \psi(x)\ \mathrm{d}x = 0$. Using the fact that ρ^s is a solution to the stationary equation (8), that is,

$$[\rho^s\ G_{\rho^s}]_x + \frac{\sigma^2}{2}\ \rho^s_{xx} = 0,$$

and inserting $\rho = \psi + \rho^s$ into equation (6), we obtain

$$\psi_t = [\psi\ (w \star \psi + G_{\rho^s})]_x + [\rho^s\ (w \star \psi)]_x + \frac{\sigma^2}{2}\ \psi_{xx}.$$

Multiplying this equation by ψ and integrating by part over $\tilde{X}$, we obtain (the extra terms are zero due to periodicity)

$$\begin{aligned}
&\frac{1}{2}\frac{\mathrm{d}}{\mathrm{d}t}\|\psi\|^2_{L^2} + \frac{\sigma^2}{2}\|\psi_x\|^2_{L^2} \\
&\leq \left|\int_{\tilde{X}} \psi_x\ \psi\ (w \star \psi + G_{\rho^s})\ \mathrm{d}x\right| + \left|\int_{\tilde{X}} \psi_x\ \rho^s\ (w \star \psi)\ \mathrm{d}x\right| \\
&\leq \left(\|w \star \psi\|_{L^\infty} + \|G_{\rho^s}\|_{L^\infty}\right)\ \|\psi_x\|_{L^2}\ \|\psi\|_{L^2} \\
&\quad + \|\rho^s\|_{L^\infty}\ \|\psi_x\|_{L^2}\ \|w \star \psi\|_{L^2}. \qquad (39)
\end{aligned}$$

Now, from inequality (12) in Lemma III.1, we have

$$\begin{aligned}
\|w \star \psi\|_{L^\infty} &\leq 2R\ \|\psi\|_{L^1(X)} \\
&\leq 2R\ \left(\|\rho\|_{L^1(X)} + \|\rho^s\|_{L^1(X)}\right) = 4R,
\end{aligned}$$

and

$$\|G_{\rho^s}\|_{L^\infty} \leq 2R\left(\|\rho^s\|_{L^1(X)} + M\right) = 2R(1 + M).$$

Also, following a similar procedure as in (35) and (36) with $M = 0$, we obtain $\|w \star \psi\|_{L^2} \leq (2R^2/\sqrt{3})\ \|\psi\|_{L^2}$. Finally, from (28) in Lemma IV.2, we have $\|\rho^s\|_{L^\infty} \leq \mathrm{e}^{8R(1+M)/\sigma^2}$. To save space, let us define

$$\alpha \coloneqq 2R(3 + M) + (2R^2/\sqrt{3})\,\mathrm{e}^{8R(1+M)/\sigma^2}. \qquad (40)$$

Using these estimates and the Young's inequality, we can rewrite (39) as

$$\begin{aligned}
\frac{1}{2}\frac{\mathrm{d}}{\mathrm{d}t}\|\psi\|^2_{L^2} + \frac{\sigma^2}{2}\|\psi_x\|^2_{L^2} &\leq \alpha\ \|\psi_x\|_{L^2}\|\psi\|_{L^2} \\
&\leq \frac{\alpha^2}{\sigma^2}\|\psi\|^2_{L^2} + \frac{\sigma^2}{4}\|\psi_x\|^2_{L^2}.
\end{aligned}$$

Hence,

$$\frac{1}{2}\frac{\mathrm{d}}{\mathrm{d}t}\|\psi\|^2_{L^2} \leq \frac{\alpha^2}{\sigma^2}\|\psi\|^2_{L^2} - \frac{\sigma^2}{4}\|\psi_x\|^2_{L^2}.$$

Once again, since $\int_{\tilde{X}} \psi(x)\ \mathrm{d}x = 0$, we can use the Poincaré inequality $\|\psi\|_{L^2} \leq C\ \|\psi_x\|_{L^2}$ with optimal Poincaré constant $C = 1/\pi$, to obtain

$$\frac{\mathrm{d}}{\mathrm{d}t}\|\psi\|^2_{L^2} \leq \left(\frac{2\alpha^2}{\sigma^2} - \frac{\pi^2\sigma^2}{2}\right)\|\psi\|^2_{L^2}.$$

Then, by Grönwall's inequality, we have

$$\|\psi(t)\|^2_{L^2} \leq \|\psi(0)\|^2_{L^2} \exp\left\{\left(\frac{2\alpha^2}{\sigma^2} - \frac{\pi^2\sigma^2}{2}\right)t\right\}.$$

Now, notice that $\|\psi(0)\|_{L^2} \leq \|\rho_0\|_{L^2} + \|\rho^s\|_{L^2}$ is finite. Thus, if the constant factor in the exponential is negative, then $\|\psi(t)\|^2_{L^2} \to 0$ as $t \to \infty$. Negativity of the this constant factor corresponds to the condition $\sigma > \sigma_s$, where $\sigma_s > 0$ solves (10) – the object α is defined in (40). □

V. Clustering Behavior: Fourier Analysis

In this section, we exploit the periodic nature of the system and use Fourier analysis to study the behavior of the solution to the PDE (6) with *uniform initial condition* $\rho_0 = 1$. To this end, we derive a system of ordinary differential equations (ODEs) describing the evolution of Fourier coefficients of the normal opinion density ρ. These ODEs are then used to provide an approximation scheme for characterizing the initial clustering behavior of the system including the number and the timing of possible clusters. This numerical scheme is in essence similar to the linear stability analysis previously employed by [37], [40], [43], [53], [63] for analysis of noisy bounded confidence models without radicals.

A. Finite-dimensional Approximation in Frequency Domain

Notice that the set $\{\cos(\pi n x)\}_{n=0}^{\infty}$ is an orthogonal basis for the space $L^2_{ep}(\tilde{X})$ containing even 2-periodic functions on $\tilde{X} = [-1, 1]$. Then, the even 2-periodic extension of the probability densities in the model allows us to consider the Fourier expansions of ρ and ρ_r in the form of

$$\begin{cases} \rho(x,t) = \sum_{n=0}^{\infty}\ p_n(t)\ \cos(\pi n x), \\ \rho_r(x) = \sum_{n=0}^{\infty}\ q_n\ \cos(\pi n x). \end{cases} \qquad (41)$$

By inserting the expansions (41) into (6) and setting the inner product of the residual with elements of the basis to zero (in other words, taking inverse Fourier transform), we can obtain a system of quadratic ODEs describing the evolution of Fourier coefficients $p_n(t)$. Considering the first frequency components $n = 1, \ldots, N_f$, these ODEs are expressed as

$$\dot{p}_n = c_n + b_n^T p + p^T Q_n p, \qquad (42)$$

where $p = (p_1, p_2, \ldots, p_{N_f})^T$. Note that for $n = 0$, i.e., the constant term in the Fourier expansion, we obtain $\dot{p_0} = 0$. This is due to the periodic nature of the system that preserves the zeroth moment. The coefficients in (42) are given by

$$\begin{aligned}
&c_n = 2MRf_nq_n, \\
&(b_n)_k = \begin{cases} 2Rf_n + \frac{MR}{2}f_{2n}q_{2n} - \frac{\pi^2\sigma^2n^2}{2}, & k = n \\ nMR(g_{n+k} + g_{n-k}), & k \neq n, \end{cases} \\
&(Q_n)_{k,l} = \begin{cases} nRf_k/k, & l = n - k > 1 \\ nR\left(\frac{f_k}{k} + \frac{f_{n-k}}{n-k}\right), & l = k - n > 1 \\ 0, & \text{otherwise}, \end{cases}
\end{aligned} \qquad (43)$$

where $f_i \coloneqq -\cos(\pi i R) + \operatorname{sinc}(\pi i R)$ and $g_i \coloneqq q_{|i|}f_i/i$, with $\operatorname{sinc} x = \sin x/x$. Recall that $q_n, n \in \mathbb{N}$ are the Fourier coefficients of ρ_r.

B. Initial Clustering Behavior

The possible clustering behavior of noisy interacting particle systems is known to mainly depend on the noise level. That is, for noises larger than a critical level, the random drifts due to noise are expected to overcome the attractive forces among the agent and suppress clustering behaviors; see Fig. 2a for numerical simulations of the model under study for increasing levels of noise. A detailed discussion on this phenomenon commonly known as order-disorder transition for the system under study is provided in [60, Sections 5.2 and 6.2].

For noises smaller than the critical level corresponding to order-disorder transition, agents start to form clusters. Here, we are interested in the characterization of this initial clustering behavior. To this end, we make use of the *exponential growth rate* $\gamma_n := (b_n)_n$ and *linear growth rate* c_n given in (43). The proposed numerical method is as follows. We ignore the interactions between different frequencies in (42), that is, for each frequency $n = 1\ldots, N_f$, we consider the equation $\dot{p}_n = c_n + \gamma_n p_n$ with $p_n(0) = 0$ for initial evolution of the Fourier coefficient p_n. Then, for a given set of model parameters (σ, R, M) and radical opinions density ρ_r, we numerically compute the *dominant wave-number* $n^* := \operatorname{argmax}_{n\in\mathbb{N}} \gamma_n$ with $\gamma_{n^*} > 0$, that is, the unstable mode with the largest exponential growth rate. We speculate that the corresponding trigonometric term $p_{n^*}\cos(\pi n^* x)$ is the dominant component of the initial clustering behavior. The sign of p_{n^*} depends on the linear growth rate c_{n^*}: $p_{n^*} > 0$ if $c_{n^*} > 0$, and $p_{n^*} < 0$ otherwise.

Considering the even 2-periodic extension of the model, the dominant wave-form must be interpreted on the interval $\tilde{X} = [-1, 1]$. Then, the *number of initial clusters* n_{clu} in the interval $X = [0, 1]$, resulting from the wave-form $1 + p_{n^*}\cos(\pi n^* x)$, is given by

$$n_{\text{clu}} := \begin{cases} \lfloor \frac{n^*}{2} \rfloor + 1, & c_{n^*} > 0 \\ \lceil \frac{n^*}{2} \rceil, & c_{n^*} < 0. \end{cases} \tag{44}$$

We also expect that the timing of this initial clustering behavior to be inversely related to the corresponding exponential growth rate γ_{n^*}. Indeed, by solving for the time for which the solution to the equation $\dot{p}_n = c_n + \gamma_n p_n$ is equal to ± 1, we can approximate the *time to initial clustering* t_{clu} as

$$t_{\text{clu}} := \frac{1}{\gamma_{n^*}} \ln\left(1 + \frac{\gamma_{n^*}}{|c_{n^*}|}\right). \tag{45}$$

A similar approximation has been used in [53] in order to derive the time to the initial clustering using fluctuation theory.

VI. Numerical Study

In this final section, we provide a numerical study of the model at hand for a particular distribution of radical agents/opinions through simulations of the corresponding discrete- and continuum-agent models. In particular, we validate the result of Fourier analysis for characterization of initial clustering behavior presented in Section V-B.

A. Set-up

The particular radical distribution considered in this section is a triangular distribution with average A and width $2S$

$$\rho_r(x) = \frac{S - |x - A|}{S^2} \text{ for } |x - A| \le S,\ 0 \text{ otherwise.} \tag{46}$$

Although this choice may seem specific, it is rich enough for our purposes. In particular, with this choice, the zeroth, first and second moments of the radical opinions density are simply captured by the parameters M, A and S, respectively. Moreover, we assume that the radicals are concentrated around their average opinion, that is, we consider small values of S (w.r.t. the confidence range R).

For the discrete-agent model, the SDEs (4) are solved numerically using the Euler-Maruyama method for $N = 500$ normal agents with time step $\Delta t = 0.01$. In particular, for the radical agents, we produce a random sample of size $N_r = MN$ from the triangular distribution (46). The initial distribution of normal agents is taken to be uniform, that is, the initial opinions are randomly sampled from a uniform distribution on the interval $X = [0, 1]$. For complete correspondence between the discrete- and continuum- agent models, we also consider the effect of even 2-periodic extension in the simulations of the discrete-agent model.

For numerical simulation of the continumm-agent model described by PDF (6), we use the ODEs (42) to compute the coefficients of Fourier expansion of normal opinion density ρ using the first $N_f = 128$ terms of the expansion. However, regarding the radical opinion density, one notices that the considered triangular distribution does not satisfy the conditions of Theorem II.1 for well-posedness of PDE (6), that is $\rho_r \notin H^2_{ep}(\tilde{X})$. This will not be an issue since we will be working with the projection of the proposed ρ_r in the Hilbert space $L^2_{ep}(\tilde{X})$. That is, we use the Fourier coefficients of ρ_r in (42), which for the triangular distribution (46) are given by

$$q_n = 2\cos(n\pi A)\,\operatorname{sinc}^2(n\pi S/2). \tag{47}$$

To be precise, we need the Fourier coefficients q_n of ρ_r for $1 \le n \le 2N_f$, that is, twice the length of Fourier expansion of ρ; see the linear terms of (42). For the initial condition, we again consider uniform distribution $\rho_0 = 1$, which corresponds to $p_0 = 1$ and $p_n(0) = 0$ for the Fourier coefficients. A detailed description of the numerical scheme for simulation of the discrete- and continuum-agent models is provided in [60, Section 6].

In the sequel, we use the *order parameter*

$$Q_d(t) = N^{-2}\textstyle\sum_{i,j=1}^{N} \mathbf{1}_{|x_i(t)-x_j(t)|\le R},$$

introduced in [43] and its continuum counterpart

$$Q_c(t) = \textstyle\int_{X^2} \rho(x,t)\rho(y,t)\mathbf{1}_{|x-y|\le R}\,\mathrm{d}x\mathrm{d}y,$$

to quantify orderedness in the clustering behavior of the model. In particular, we use the evolution of the order parameter for a better characterization of the *timing* of the clustering behavior in the simulation results. In words, the order parameter Q is the (normalized) number/mass of agents that are in R-neighborhood of and hence interacting with each other. In particular, in the continuum case, $Q_c = 2R$ for a uniform

distribution of opinions (absolute disorder), while $Q_c = 1$ for a single-cluster distribution with all agents residing in an interval of width R or less (complete order). In case of a clustered behavior, roughly speaking, the inverse of the order parameter is equal to the *number of clusters*. For instance, the $2R$-conjecture [42], [43] states that for a noiseless system without radicals and starting from a uniform initial distribution ($Q = 1$), the dynamics will converge to a clustered profile with the distance between clusters being (approximately) $2R$, or equivalently, with $\frac{1}{2R}$ clusters ($Q \approx 2R$). In presence of noise, however, the system experiences a phase transition (order-disorder transition) depending on the noise level [43], [53]. In particular, for noises larger than a critical level (depending on R), the clustering behavior disappears and the system converges to a (somewhat) uniform state with $Q \approx 1$. As shown in Fig. 2b, the same transition occurs in noisy systems in presence of radicals, considered in this study.

In all the simulation results reported in this section the width of radicals distribution and the confidence range are fixed at $S = 0.1$ and $R = 0.1$, respectively.

B. Initial Clustering Behavior

For sufficiently small noises, agents start to form clusters; see Figs. 2 and 3. In particular, we observe a cluster of normal agents around the average radical opinion A due to the force field generated by the radicals. Generally, three types of clusters may form: (1) the cluster at the average radical opinion A, (2) the cluster(s) at the extreme opinions $x = 0$ or (and) $x = 1$, and (3) the cluster(s) around opinion values other than $x = 0, 1, A$. The third type of clusters are expected to perform a random walk with their center of mass moving like a Brownian motion (assuming clusters do not interact). The effective diffusivity of these Brownian motions is inversely related to the size of the cluster, i.e., the number of agents in the cluster. This will result in a process of consecutive merging between these clusters until complete disappearance of them. Detailed descriptions of this process are provided in [43], [53]. Notice, however, that this description does not apply to cluster(s) formed at $x = A$ and $x = 0, 1$. These clusters are affected by forces other than the normal attractions among the agents within the cluster. The cluster formed at $x = A$ is under influence of radicals and the possible clusters at the extreme opinions $x = 0, 1$ are reinforced due to the even 2-periodic extension considered in our model. The behavior of these clusters (survival or dissolution) depends on their size, the exogenous force acting on them, and the effect of other clusters in their neighborhood.

We now use the analysis scheme provided in Section V-B to investigate the effect of the zeroth and first moment of radicals (M and A, respectively) on the initial clustering behavior of the model for noises smaller than the critical level. In particular, we investigate the effect of M and A on the number, position and timing of initial clusters for different values of σ. We again emphasize that we are considering a concentrated triangular distribution for radical agents and a uniform initial distribution for normal agents.

Following the provided scheme in Section V-B, we can compute the dominant wave-number n^*, number of initial clusters n_{clu}, and time to initial clustering t_{clu} for a general combination of model parameter (σ, M, A) (recall that we fixed $R = S = 0.1$). A detailed illustrative example on this process is provided in [60, Section 6.3.1]. Fig. 4 shows the result of this analysis for different values of M and A at three different noise levels σ. Here, we only consider the values $A < 1 - R = 0.9$ since for $1 - R < A < 1$ the boundary effect due to even 2-periodic extension comes into play.

Comparing the left, middle and right panels of Fig. 4 for different levels of noise, the analysis shows that as the level of noise increases, the number of clusters in the possible clustering behavior of the system is expected to decrease (see Fig. 4b), while the timing experiences a general increase (see Fig. 4c). In particular, with respect to the timing, we notice that as the level of noise decreases, the initial clustered profile is expected to emerge faster. Indeed, these effects can be seen in the simulation results depicted in Fig 2b.

For low levels of noise, e.g., $\sigma = 0.01$ (see the left panels in Fig. 4), the analysis shows that the dominant wave-number does not depend on the M or A. However, both M and A are expected to affect the the timing of the initial clustering behavior. In particular, as M increases, t_{clu} decreases. Fig. 3 shows the simulation results for $\sigma = 0.01$ and compares the evolution of opinions for different values of M and A. For the continuum model in the the top panels of Fig. 3, we observe that a 4-cluster profile has emerged in all systems, while the analysis predicts a 4-cluster profile for $\mathcal{S}_1$ and $\mathcal{S}_2$ and a 5-cluster profile for $\mathcal{S}_3$ for the initial clustering (see the left panel of Fig. 4b). Moreover, comparing Figs. 3a and 3b shows that M only affects the timing of clustering behavior. This effect is better seen in Fig. 3g, where we observe a faster convergence of order parameter for $\mathcal{S}_2$ with larger M. On the other hand, comparing Figs. 3b and 3c corresponding to $A = 0.85$ and $A = 0.7$, respectively, we observe that the first moment of radical opinions density A mainly affects the position of clusters. That is, the clustered profile emerges in a way that we observe a particular cluster formed at the average radical opinion A.

Monte Carlo simulations of the discrete-agent model reveal that the same general description also holds for this system. This is particularly seen in the time evolution of the order parameter in the discrete-agent model as depicted in Fig. 3h. However, we note that there are differences between the behavior of the continuum- and discrete-agent models. First, we observe an almost uniform distribution of normal agents in the opinion range $[0.1; 0.5]$ in the middle panels of Fig. 3 for the discrete-agent model. This is due to the fact that the exact position of the corresponding clusters formed in the discrete-agent model varies within this range. Individual realizations of the discrete model show one, two or three clusters in this range. This effect can be clearly seen in the top panel of Fig. 2a for $\sigma = 0.01$, and has also been reported by [37] in Monte Carlo simulations of a noisy Defuant model. More importantly, the evolution of order parameter in Fig. 3g shows that the continuum-agent model has seemingly converged to steady-state with four clusters, while this is clearly not the case for the discrete-agent model as can be seen in Fig. 3h. Indeed, in the discrete-agent model, as described in the beginning of

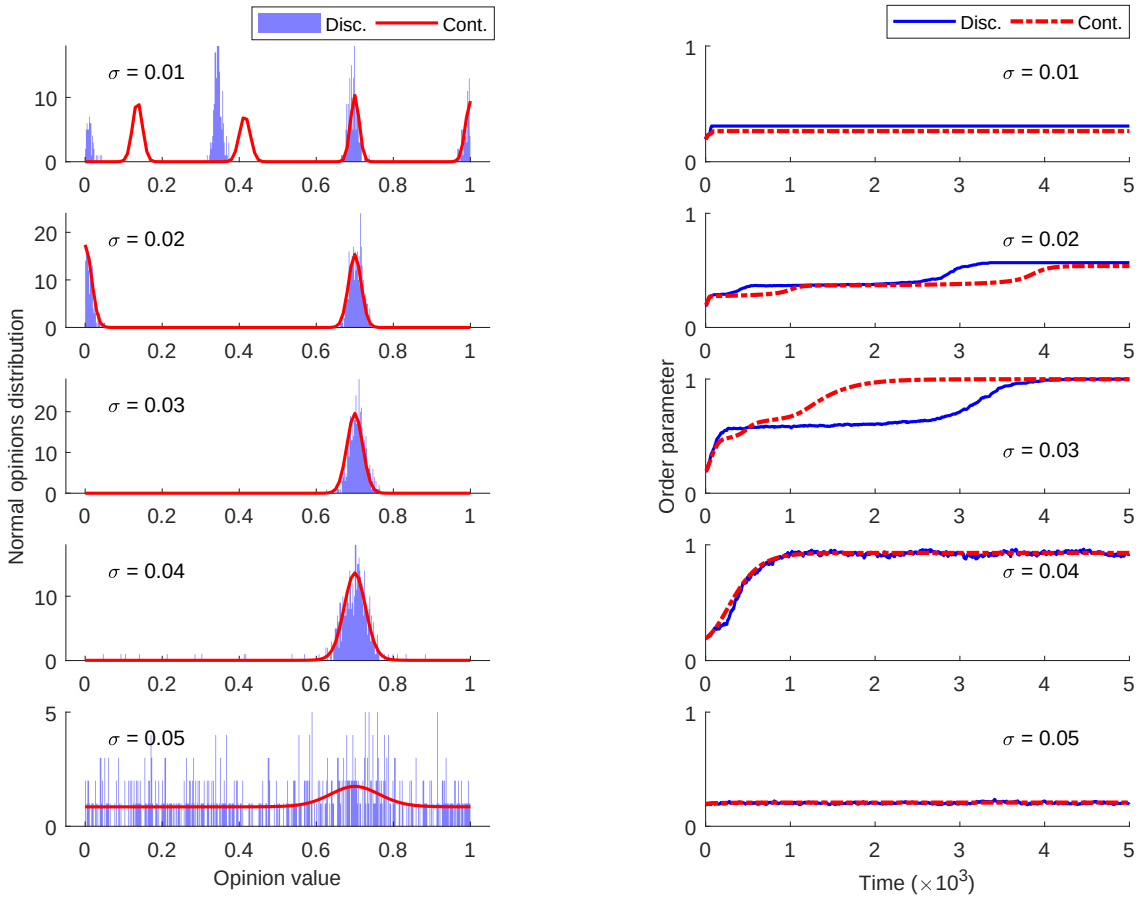

(a) Distribution of opinions/agents at $t = 10^4$

(b) Evolution of the order parameter

Fig. 2. Numerical simulation of the discrete-agent model (*Disc.*) and continuum-agent model (*Cont.*) for different values of noise σ with model parameters $(R, M) = (0.1, 0.1)$. The initial distribution of normal agents/opinions is taken to be normal and the distribution of radical agent/opinions is the triangular distribution of (46) with $(A, S) = (0.7, 0.1)$. As noise increases the number of clusters decreases so that for a large enough noise (e.g., $\sigma = 0.05$) the clustering behavior almost disappears (order-disorder transition). Moreover, in case of a clustered profile, the inverse of the order parameter is equal to the number of clusters; e.g., for $\sigma = 0.03$ the system first forms a 2-cluster profile (the flat area with order parameter around 0.5), and then converges to a single-cluster profile (with order parameter equal to one).

this section, all the possible clusters formed around opinion values other than $x = 0, 1, A$ will necessarily disappear in the steady state profile, where the time required for their disappearance depends on the noise level and particularly the size of these clusters. Hence, unlike the discrete-agent model, for the continuum-agent model (in the limit $N \to \infty$), the system may require *infinite time* for this merging of the clusters to occure. This, in turn, can lead to differet behaviors in the discrete- and continuum-agent models over exponentially large times scales [43]; see also [60, Section 6].

As shown in Fig. 4, for higher levels of noise, e.g., $\sigma = 0.03$, we observe nonlinear effects. That is, M and A start to affect the dominant wave-number (see the middle and right panels of Fig. 4a). Nevertheless, these effects are limited as the number of clusters is still 3 or 4 for $\sigma = 0.02$ and 2 or 3 for $\sigma = 0.03$. Besides, we still observe a general increase in the timing of the clustering behavior as M decreases. Numerical simulations of the model for $\sigma = 0.03$ are also in general agreement with these predictions (results not shown here, see [60, Section 6.3.2]).

To summarize the discussions above, for concentrated distribution of radicals, the main effect of the zeroth and first moments of radical distribution is on the timing and positioning of the possible clustering behavior, respectively. The number of clusters (to be precise, the life-time of possible transient clustered profiles) is mainly determined by the noise level of the system. This is particularly the case for lower levels of noise.

Appendix A
Preliminaries on Function Spaces

The definitions provided in this section are mostly borrowed from [61]. Let $\{f_k\}_{k=1}^{\infty}$ be a sequence in a Banach space B with norm $\|\cdot\|_B$. The *strong* convergence $f_k \to f$ implies $\|f_k - f\|_B \to 0$, while the *weak* convergence $f_k \rightharpoonup f$ implies $g(f_k) \to g(f)$ for all bounded linear functionals $g : B \to \mathbb{R}$.

Let $f : \tilde{X} \to \mathbb{R}$ be a measurable function on $\tilde{X} = (-1, 1)$. The L^p-norm of f is defined as follows

$$\|f\|_{L^p(\tilde{X})} = \begin{cases} \left(\int_{\tilde{X}} |f(x)|^p\right)^{\frac{1}{p}}, & 1 \le p < \infty \\ \text{ess sup}_{\tilde{X}} |f(x)|, & p = \infty. \end{cases}$$

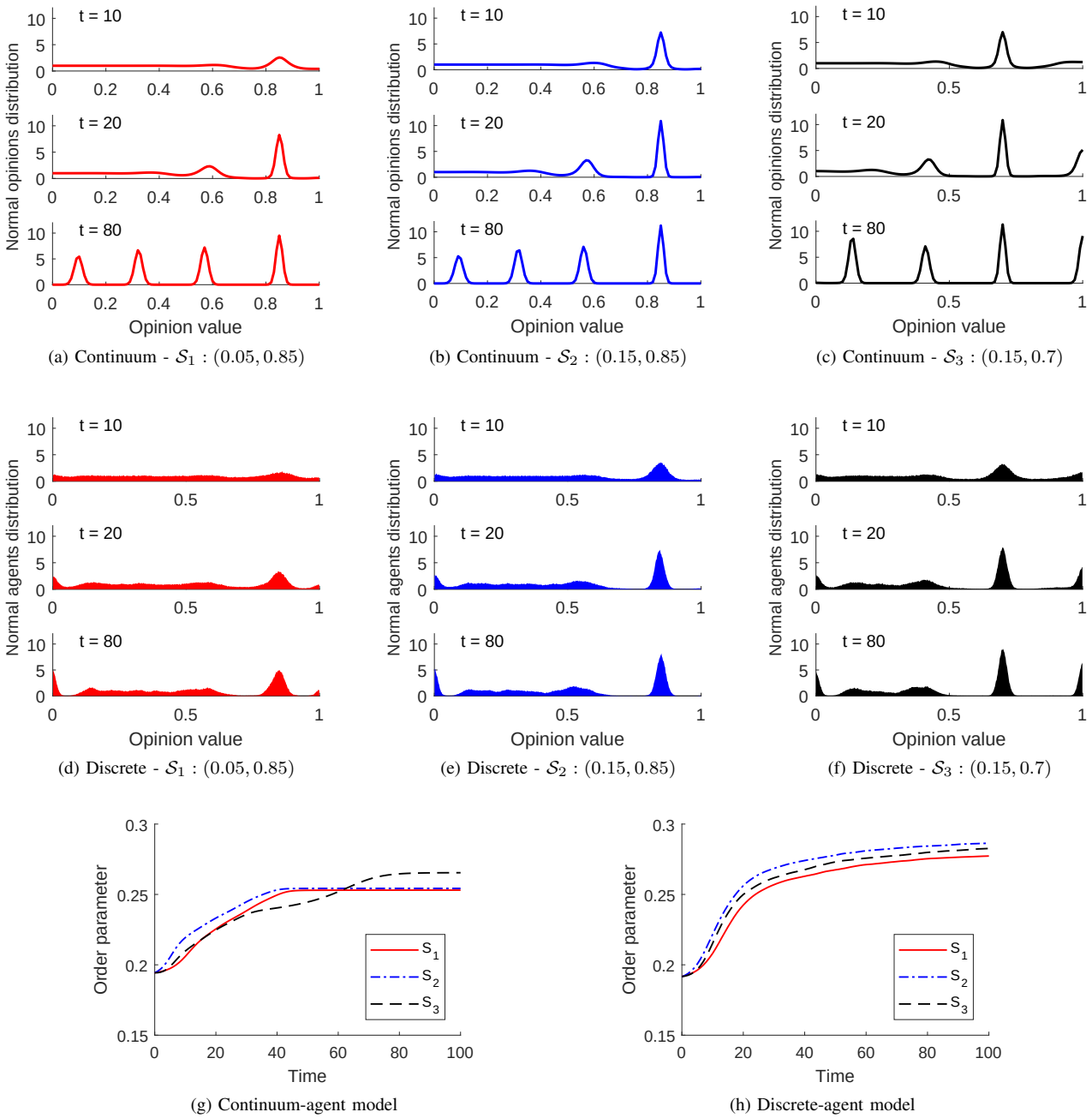

(a) Continuum - $\mathcal{S}_1 : (0.05, 0.85)$ (b) Continuum - $\mathcal{S}_2 : (0.15, 0.85)$ (c) Continuum - $\mathcal{S}_3 : (0.15, 0.7)$

(d) Discrete - $\mathcal{S}_1 : (0.05, 0.85)$ (e) Discrete - $\mathcal{S}_2 : (0.15, 0.85)$ (f) Discrete - $\mathcal{S}_3 : (0.15, 0.7)$

(g) Continuum-agent model (h) Discrete-agent model

Fig. 3. Numerical simulation of the model with $\sigma = 0.01$ for different values of (M, A), namely, $\mathcal{S}_1 : (0.05, 0.85)$, $\mathcal{S}_2 : (0.15, 0.85)$, and $\mathcal{S}_3 : (0.15, 0.7)$. The upper panels (a, b, and c) show the opinion distribution for continuum-agent model. The middle panels (d, e, and f) show the the result of Monte Carlo simulation (average of 300 realizations) of discrete-agent model. The lower panels (g and h) show the evolution of order parameter for these systems.

$L^p(\tilde{X})$ denotes the Banach space of all measurable functions $f : \tilde{X} \to \mathbb{R}$ for which $\|f\|_{L^p(\tilde{X})} < \infty$.

Let $f, g \in L^1_{loc}(\tilde{X})$ be locally summable functions (i.e., f, g have a finite integral over every compact subset of $\tilde{X}$). We say that g is the k-th *weak* (partial) derivative of f, if

$$\int_{\tilde{X}} f \, \partial_x^k \phi \, \mathrm{d}x = (-1)^k \int_{\tilde{X}} g \, \phi \, \mathrm{d}x,$$

for all test functions $\phi \in C_c^\infty(\tilde{X})$ (infinitely differentiable functions $\phi : \tilde{X} \to \mathbb{R}$ with compact support in $\tilde{X}$).

$H^k(\tilde{X})$ for $k \in \mathbb{N}$ is used to denote the Sobolev space $W^{k,2}(\tilde{X})$ consisting of functions $f \in L^2(\tilde{X})$ whose *weak* derivatives up to order k exist and belong to $L^2(\tilde{X})$. Note that $H^k(\tilde{X})$ is a Hilbert space.

We use the subscript *per* to denote the closed subspace of *periodic* functions in the corresponding function space, e.g.,

$$L^p_{per}(\tilde{X}) = \{f \in L^p(\tilde{X}) : f(-1) = f(1)\},$$
$$H^k_{per}(\tilde{X}) = \{f \in H^k(\tilde{X}) : f(-1) = f(1)\}.$$

Similarly, we use the subscript *ep* to denote the closed subspace of *even periodic* functions in the corresponding function

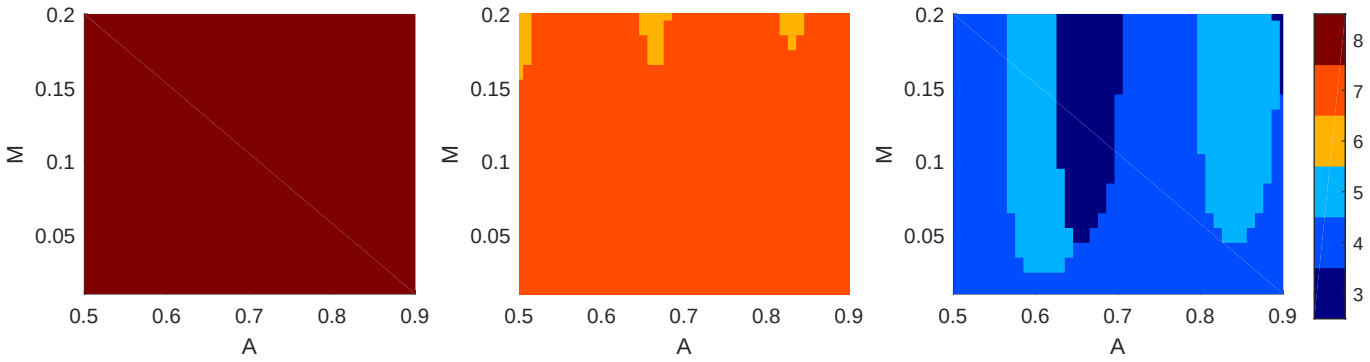

(a) Dominant wave-number: n^*

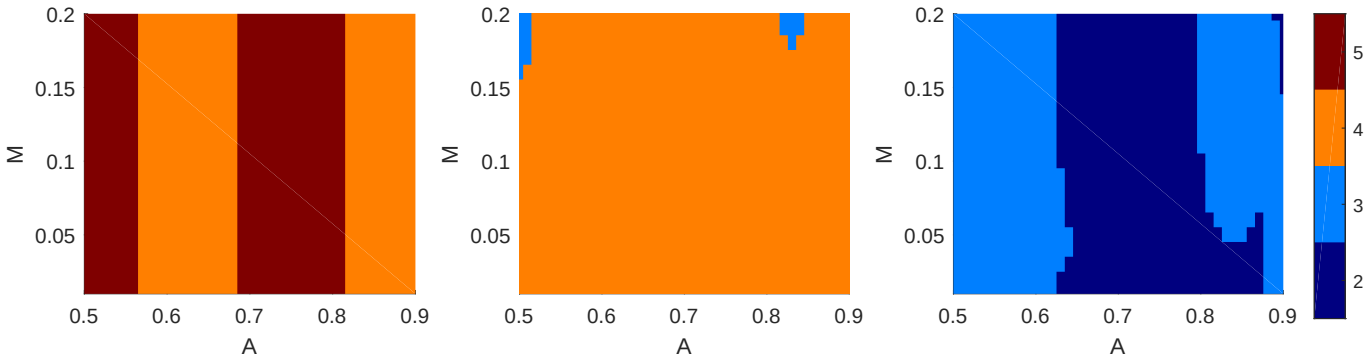

(b) Number of initial clusters: n_{clu}

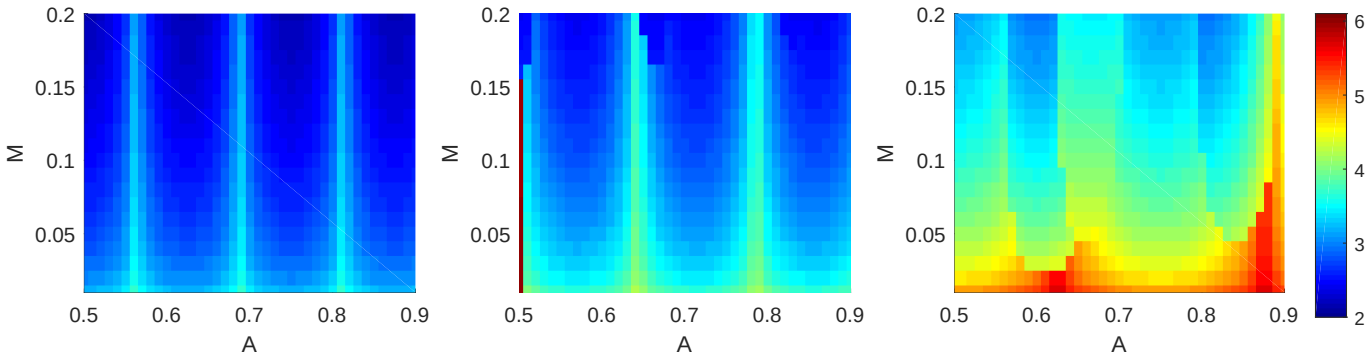

(c) Time to initial clustering: $\ln(t_{\text{clu}})$

Fig. 4. Characterization of the initial clustering behavior based on the dominant wave-number in the Fourier expansion of the continuum-agent model for different values of M and A with noise levels $\sigma = 0.01$ (left column), $\sigma = 0.02$ (middle column), and $\sigma = 0.03$ (right column).

space, e.g.,

$$L^p_{ep}(\tilde{X}) = \{f \in L^p_{per}(\tilde{X}) : f(-x) = f(x),\ \forall x \in \tilde{X}\},$$
$$H^k_{ep}(\tilde{X}) = \{f \in H^k_{per}(\tilde{X}) : f(-x) = f(x),\ \forall x \in \tilde{X}\}.$$

We denote the dual space of $H^1_{per}(\tilde{X})$ by $H^{-1}_{per}(\tilde{X})$, that is, the space of bounded linear functionals on $H^1_{per}(\tilde{X})$. Moreover, we use $\langle \cdot, \cdot \rangle$ to denote the corresponding paring of $H^1_{per}(\tilde{X})$ and $H^{-1}_{per}(\tilde{X})$. That is, for $f \in H^1_{per}(\tilde{X})$ and $g \in H^{-1}_{per}(\tilde{X})$, we use $\langle g, f \rangle$ to denote the real number $g(f)$. Since periodic boundary condition allows for integration by parts without extra terms, $H^{-1}_{per}(\tilde{X})$ has most of the properties of the space $H^{-1}(\tilde{X})$, the dual space of $H^{-1}_0(\tilde{X})$; see [61, Section 5.9.1] for a detailed description of the space $H^{-1}(\tilde{X})$.

REFERENCES

[1] S. Boccaletti, V. Latora, Y. Moreno, M. Chavez, and D.-U. Hwanga, "Complex networks: Structure and dynamics," *Physics Reports*, vol. 424, no. 4–5, pp. 175–308, 2006.

[2] Y.-Y. Liu and A.-L. Barabási, "Control principles of complex systems," *Reviews of Modern Physics*, vol. 88, p. 035006, 2016.

[3] S. H. Strogatz, *Sync: The Emerging Science of Spontaneous Order*. New York: Hyperion Press, 2003.

[4] C. W. Wu, *Synchronization in Complex Networks of Nonlinear Dynamical Systems*. Singapore: World Scientific, 2007.

[5] M. Mesbahi and M. Egerstedt, *Graph Theoretic Methods in Multiagent Networks*. Princeton and Oxford: Princeton University Press, 2010.

[6] A. Pogromsky, G. Santoboni, and H. Nijmeijer, "Partial synchronization: from symmetry towards stability," *Physica D: Nonlinear Phenomena*, vol. 172, no. 1, pp. 65 – 87, 2002.

[7] W. Wu, W. Zhou, and T. Chen, "Cluster synchronization of linearly coupled complex networks under pinning control," *IEEE Transactions*

on Circuits and Systems I: Regular Papers, vol. 56, no. 4, pp. 829–839, 2009.

[8] W. Xia and M. Cao, "Clustering in diffusively coupled networks," *Automatica*, vol. 47, no. 11, pp. 2395–2405, 2011.

[9] L. Pecora, F. Sorrentino, A. Hagerstrom, T. Murphy, and R. Roy, "Cluster synchronization and isolated desynchronization in complex networks with symmetries," *Nature Communications*, vol. 5, p. 4079, 2014.

[10] L. Lu, C. Li, S. Bai, L. Gao, L. Ge, and C. Han, "Cluster synchronization between uncertain networks with different dynamics," *Physica A*, vol. 469, pp. 429 – 437, 2017.

[11] R. Abelson, "Mathematical models of the distribution of attitudes under controversy," in *Contributions to Mathematical Psychology*, N. Frederiksen and H. Gulliksen, Eds. New York: Holt, Rinehart & Winston, Inc, 1964, pp. 142–160.

[12] T. Kurahashi-Nakamura, M. Mäs, and J. Lorenz, "Robust clustering in generalized bounded confidence models," *Journal of Artificial Societies and Social Simulation*, vol. 19, no. 4, p. 7, 2016.

[13] N. Friedkin, "The problem of social control and coordination of complex systems in sociology: A look at the community cleavage problem," *IEEE Control Systems Magazine*, vol. 35, no. 3, pp. 40–51, 2015.

[14] C. Castellano, S. Fortunato, and V. Loreto, "Statistical physics of social dynamics," *Reviews of Modern Physics*, vol. 81, pp. 591–646, 2009.

[15] H. Xia, H. Wang, and Z. Xuan, "Opinion dynamics: A multidisciplinary review and perspective on future research," *International Journal of Knowledge and Systems Science*, vol. 2, no. 4, pp. 72–91, 2011.

[16] D. Acemoglu and A. Ozdaglar, "Opinion dynamics and learning in social networks," *Dynamic Games and Applications*, vol. 1, pp. 3–49, 2011.

[17] A. Proskurnikov and R. Tempo, "A tutorial on modeling and analysis of dynamic social networks. Part I," *Annual Reviews in Control*, vol. 43, 2017, 65-79.

[18] ——, "A tutorial on modeling and analysis of dynamic social networks. Part II," *Annual Reviews in Control*, vol. 45, 2018, 166–190.

[19] A. V. Proskurnikov, C. Ravazzi, and F. Dabbene, "Dynamics and structure of social networks from a systems and control viewpoint: A survey of Roberto Tempo's contributions," *Online Social Networks and Media*, vol. 7, pp. 45 – 59, 2018.

[20] L. Mastroeni, P. Vellucci, and M. Naldi, "Agent-based models for opinion formation: A bibliographic survey," *IEEE Access*, vol. 7, pp. 58 836–58 848, 2019.

[21] A. Aydogdu, S. T. McQuade, and N. P. Duteil, "Opinion dynamics on a general compact Riemannian manifold," *Networks & Heterogeneous Media*, vol. 12, p. 489, 2017.

[22] D. Acemoglu, G. Como, F. Fagnani, and A. Ozdaglar, "Opinion fluctuations and disagreement in social networks," *Mathematics of Operations Research*, vol. 38, no. 1, pp. 1–27, 2013.

[23] J. Liu, X. Chen, T. Basar, and M. Belabbas, "Exponential convergence of the discrete- and continuous-time Altafini models," *IEEE Transactions on Automatic Control*, vol. 62, no. 12, pp. 6168–6182, 2017.

[24] M. McPherson, L. Smith-Lovin, and J. Cook, "Birds of a feather: Homophily in social networks," *Annual Review of Sociology*, vol. 27, pp. 415–444, 2001.

[25] C. G. Lord and L. Ross, "Biased assimilation and attitude polarization: The effects of prior theories on subsequently considered evidence," *Journal of Personality and Social Psychology*, vol. 37, no. 11, pp. 2098–2109, 1979.

[26] U. Krause, "A discrete nonlinear and non-autonomous model of consensus formation," *Communications in Difference Equations*, vol. 2000, pp. 227–236, 2000.

[27] G. Deffuant, D. Neau, F. Amblard, and G. Weisbuch, "Mixing beliefs among interacting agents," *Advances in Complex Systems*, vol. 3, no. 01–04, pp. 87–98, 2000.

[28] S. Motsch and E. Tadmor, "Heterophilious dynamics enhances consensus," *SIAM Review*, vol. 56, no. 4, pp. 577–621, 2013.

[29] S. R. Etesami, "A simple framework for stability analysis of state-dependent networks of heterogeneous agents," *SIAM Journal on Control and Optimization*, vol. 57, no. 3, pp. 1757–1782, 2019.

[30] B. Chazelle and C. Wang, "Inertial Hegselmann-Krause systems," *IEEE Transactions on Automatic Control*, vol. 62, no. 8, pp. 3905–3913, 2017.

[31] A. Mirtabatabaei and F. Bullo, "Opinion dynamics in heterogeneous networks: Convergence conjectures and theorems," *SIAM Journal on Control and Optimization*, vol. 50, no. 5, pp. 2763–2785, 2012.

[32] S. R. Etesami and T. Başar, "Game-theoretic analysis of the Hegselmann-Krause model for opinion dynamics in finite dimensions," *IEEE Transactions on Automatic Control*, vol. 60, no. 7, pp. 1886–1897, 2015.

[33] R. Hegselmann and U. Krause, "Truth and cognitive division of labour: First steps towards a computer aided social epistemology," *Journal of Artificial Societies and Social Simulation*, vol. 9, no. 3, p. 1, 2006.

[34] ——, "Opinion dynamics under the influence of radical groups, charismatic leaders and other constant signals: a simple unifying model," *Networks & Heterogeneous Media*, vol. 10, no. 3, pp. 477–509, 2015.

[35] Y. Zhao, L. Zhang, M. Tang, and G. Kou, "Bounded confidence opinion dynamics with opinion leaders and environmental noises," *Computers & Operations Research*, vol. 74, pp. 205–213, 2016.

[36] M. Porfiri, E. M. Bollt, and D. J. Stilwell, "Decline of minorities in stubborn societies," *The European Physical Journal B*, vol. 57, no. 4, pp. 481–486, 2007.

[37] M. Pineda, R. Toral, and E. Hernández-García, "Noisy continuous-opinion dynamics," *Journal of Statistical Mechanics: Theory and Experiment*, vol. 2009, no. 08, p. P08001, 2009.

[38] E. Ben-Naim, P. Krapivsky, and S. Redner, "Bifurcations and patterns in compromise processes," *Physica D*, vol. 183, no. 3, pp. 190–204, 2003.

[39] S. Grauwin and P. Jensen, "Opinion group formation and dynamics: Structures that last from nonlasting entities," *Physical Review E*, vol. 85, p. 066113, 2012.

[40] M. Pineda, R. Toral, and E. Hernández-García, "The noisy Hegselmann-Krause model for opinion dynamics," *The European Physical Journal B*, vol. 86, no. 12, p. 490, 2013.

[41] A. Carro, R. Toral, and M. San Miguel, "The role of noise and initial conditions in the asymptotic solution of a bounded confidence, continuous-opinion model," *Journal of Statistical Physics*, vol. 151, pp. 131–149, 2013.

[42] V. D. Blondel, J. M. Hendrickx, and J. N. Tsitsiklis, "On the 2r conjecture for multi-agent systems," in *2007 European Control Conference (ECC)*, 2007, pp. 874–881.

[43] C. Wang, Q. Li, W. E, and B. Chazelle, "Noisy Hegselmann-Krause systems: Phase transition and the 2R-conjecture," *Journal of Statistical Physics*, vol. 166, no. 5, pp. 1209–1225, 2017.

[44] M. Huang and J. H. Manton, "Opinion dynamics with noisy information," in *52nd IEEE Conference on Decision and Control*, 2013, pp. 3445–3450.

[45] W. Su, G. Chen, and Y. Hong, "Noise leads to quasi-consensus of Hegselmann–Krause opinion dynamics," *Automatica*, vol. 85, pp. 448–454, 2017.

[46] J. Lorenz, "Continuous opinion dynamics under bounded confidence: a survey," *International Journal of Modern Physics C*, vol. 18, no. 12, pp. 1819–1838, 2007.

[47] V. Blondel, J. Hendrickx, and J. Tsitsiklis, "Continuous-time average-preserving opinion dynamics with opinion-dependent communications," *SIAM Journal on Control and Optimization*, vol. 48, pp. 5214–5240, 2010.

[48] J. Hendrickx and A. Olshevsky, "On symmetric continuum opinion dynamics," *SIAM Journal on Control and Optimization*, vol. 54, no. 5, pp. 2893–2918, 2016.

[49] A. Mirtabatabaei, P. Jia, and F. Bullo, "Eulerian opinion dynamics with bounded confidence and exogenous inputs," *SIAM Journal on Applied Dynamical Systems*, vol. 13, no. 1, pp. 425–446, 2014.

[50] C. Canuto, F. Fagnani, and P. Tilli, "An Eulerian approach to the analysis of Krause's consensus models," *SIAM Journal on Control and Optimization*, vol. 50, pp. 243–265, 2012.

[51] L. Boudin and F. Salvarani, "Opinion dynamics: Kinetic modelling with mass media, application to the Scottish independence referendum," *Physica A*, vol. 444, pp. 448–457, 2016.

[52] A. Nordio, A. Tarable, C.-F. Chiasserini, and E. Leonardi, "Belief dynamics in social networks: A fluid-based analysis," *IEEE Transactions on Network Science and Engineering*, vol. 5, no. 4, pp. 276–287, 2018.

[53] J. Garnier, G. Papanicolaou, and T.-W. Yang, "Consensus convergence with stochastic effects," *Vietnam Journal of Mathematics*, vol. 45, no. 1, pp. 51–75, 2017.

[54] B. Chazelle, Q. Jiu, Q. Li, and C. Wang, "Well-posedness of the limiting equation of a noisy consensus model in opinion dynamics," *Journal of Differential Equations*, vol. 263, no. 1, pp. 365 – 397, 2017.

[55] M. A. S. Kolarijani, A. V. Proskurnikov, and P. Mohajerin Esfahani, "Long-term behavior of mean-field noisy bounded confidence models with distributed radicals," Proc. of 58th IEEE Conference on Decision and Control, pp. 6158–6163, 2019.

[56] D. A. Dawson, "Critical dynamics and fluctuations for a mean-field model of cooperative behavior," *Journal of Statistical Physics*, vol. 31, no. 1, pp. 29–85, 1983.

[57] K. Oelschlager, "A martingale approach to the law of large numbers for weakly interacting stochastic processes," *The Annals of Probability*, vol. 12, no. 2, pp. 458–479, 1984.

[58] J. Grtner, "On the McKean-Vlasov limit for interacting diffusions," *Mathematische Nachrichten*, vol. 137, no. 1, pp. 197–248, 1988.
[59] J. A. Carrillo, R. S. Gvalani, G. A. Pavliotis, and A. Schlichting, "Long-time behaviour and phase transitions for the McKean–Vlasov equation on the torus," *Archive for Rational Mechanics and Analysis*, Jul 2019. [Online]. Available: https://doi.org/10.1007/s00205-019-01430-4
[60] M. A. S. Kolarijani, A. V. Proskurnikov, and P. Mohajerin Esfahani, "Macroscopic noisy bounded confidence models with distributed radical opinions," *arXiv preprint arXiv:1905.04057*, 2019.
[61] L. Evans, *Partial Differential Equations*. American Mathematical Society, 2010.
[62] R. A. Adams and J. J. Fournier, *Sobolev Spaces*. Elsevier, 2003, vol. 140.
[63] M. Pineda, R. Toral, and E. Hernández-García, "Diffusing opinions in bounded confidence processes," *The European Physical Journal D*, vol. 62, no. 1, pp. 109–117, 2011.

Mohamad Amin Sharifi Kolarijani received the B.Sc. degree in control systems from University of Tehran, Iran, in 2011, and the M.Sc. degree in bioelectrics from Amirkabir University of Technology, Iran, in 2014. He is currently pursuing the Ph.D. degree at Delft Center for Systems and Control, Delft University of Technology, The Netherlands. His current research is mainly focused on mean-field models of interactive particle systems and fast algorithms for dynamic programming. He won the Bronze Medal of the Iranian National Olympiad in Physics in 2005, and was ranked 3rd in Iran's National Matriculation Exam for Graduate Studies in 2017.

Anton Proskurnikov (M'13, SM'18) is an assistant professor at the Department of Electronics and Telecommunications, Politecnico di Torino (Italy) and a part-time senior researcher at the Institute for Problems in Mechanical Engineering of the Russian Academy of Sciences. He received the M.Sc. ("Specialist") and Ph.D. ("Candidate of Sciences") degrees in applied mathematics from St. Petersburg State University in 2003 and 2005, respectively. He was an assistant professor and senior research at St. Petersburg State University (2003-2010), and later a postdoctoral researcher at the University of Groningen (2014-2016) and Delft University of Technology (2016-2018), The Netherlands. He is serving as Associate Editor at IEEE Transactions on Automatic Control and a member of Editorial Board of the Journal of Mathematical Sociology. His research interests include dynamics of complex networks, multi-agent systems, nonlinear control, and control applications to social and biological sciences.

Peyman Mohajerin Esfahani Peyman Mohajerin Esfahani is currently an assistant professor in the Delft Center for Systems and Control at the Delft University of Technology. Prior to joining TU Delft, he held several research appointments at EPFL, ETH Zurich, and MIT between 2014 and 2016. He received the B.Sc. and M.Sc. degrees from Sharif University of Technology, Iran, and the PhD degree from ETH Zurich. His research interests include theoretical and practical aspects of decision-making problems in uncertain and dynamic environments, with applications to control and security of large-scale and distributed systems. He was one of the three finalists for the Young Researcher Prize in Continuous Optimization awarded by the Mathematical Optimization Society in 2016, and was a recipient of the 2016 George S. Axelby Outstanding Paper Award from the IEEE Control Systems Society.